AIMS Materials Science, 9(6): 884–918.
DOI: 10.3934/matersci.2022053
Received: 09 June 2022
Revised: 29 August 2022
Accepted: 10 September 2022
Published: 07 November 2022

http://www.aimspress.com/journal/Materials

Review

Laser welding of aluminum battery tab to variable Al/Cu busbars in Li-ion battery joint

Ehsan Harati* and Paul Kah

Department of Engineering Science, University West, SE-46186 Trollhättan, Sweden

* **Correspondence:** Email: Ehsan.harati@hv.se; Tel: +46-73-494-8456.

Abstract: The trend is shifting from internal combustion engines (ICEs) to battery electric vehicles (BEVs). One of the important battery joints is battery tabs to the busbar connection. Aluminum (Al) and copper (Cu) are among the common materials for busbar and battery tab manufacturing. A wide range of research shows that the laser welding of busbar to battery tabs is a very promising technique. It can enhance the battery module's safety and reliability owing to its unique properties. The desired strength, ductility, fatigue life as well as electrical resistivity are crucial to attain in laser welding of dissimilar materials aluminum and copper in busbar to battery tab in BEVs. Therefore, an adequate understating of the principal factors influencing the Al–Cu busbar to battery tabs joint properties are of prime importance. The current review paper provides information on laser welding and laser brazing of dissimilar Al–Cu with thin thicknesses. Also, the common defects, the effect of materials properties on laser joining, and laser-materials interaction during the laser welding process are discussed. Laser process parameters adjustment (e.g., laser power or speed), laser operational mode, and proper choice of materials (e.g., base metals, alloying elements, filler metals, etc.) may enhance the joint properties in terms of mechanical and electrical properties.

Keywords: dissimilar laser welding; laser brazing; metal mixing; aluminum–copper welding; busbar to battery tabs welding

1. Introduction

A general trend is to shift away from internal combustion engines (ICE) to more environmentally-friendly battery electric vehicles (BEVs). A decrease in the prices of lithium-ion

batteries (LIB) and battery pack manufacturing, as well as government policies and subsidies, help to overcome the challenges in the BEVs market and to achieve more sustainable production and a greener environment [1–7].

Lithium-ion batteries having the highest energy density surpassing other traditional batteries are currently the best option for the BEVs. BEVs use the stored energy inside a battery pack which consists of many individual cells. The battery pack design is defined by electric circuit type (related to desired power and capacity) and reliability. The parallel connection secures reliability while increasing the complexity and production cost. The series connection in batteries leads to attaining the same capacity while providing a higher power. To acquire the desired properties, a combination of series and parallel connections is typically used in the car industry [8].

To evaluate joint properties and joining technology for battery interconnections appropriately, the following requirements can be defined [9]: Electrical and thermal aspects, material and metallurgical aspects, mechanical aspects, initial process parameters variations, and economic considerations. Therefore, to achieve a desirable battery joint with high strength, long fatigue life, reduced IMCs, low corrosion risk, adaptability to many surfaces and conditions, as well as low production cost, and suitability for mass production, some stress aging factors should be tackled. These stress aging factors may reduce expected battery life and performance, or even may cause short circuits and fire [10]. From the mechanical aspect dealing with dynamic loading, random vibration, and fatigue in joints adequately is of high importance. Generated heat during charging and discharging due to thermal resistance in joints, specifically in dissimilar materials e.g., Al–Cu joints, may result in dimensional changes and thus the introduction of thermal fatigue in long-term applications [11]. Also, fatigue progression can increase the electrical connection resistance [12]. Also, heating may lead to faster cell degradation, aging, thermal runaway, fire, and even explosion [13–15]. In addition, corrosion, oxidation, fretting, and intermetallic compounds (IMCs) between dissimilar materials are among many metallurgical challenges to be prevented.

Initial process parameters variations [16] such as variation in battery cell capacity in a battery module, internal resistance, connection resistance, and the cooling system immediately lead to a different current rate. This effect is more pronounced in parallel joints. Variation in initial process parameters may occur because of variation in battery chemistry and manufacturing [17], joint materials, and/or joining processes [18]. Current alongside other stress aging factors can intensify the deterioration over a long period which leads to inconsistency in the degradation and even a stronger overall degradation of battery cells. All the above-mentioned aging factors, e.g., energy loss and heat generation because of electrical resistance, in the battery joints, lead to less battery module capacity and power and thus shortened “driving range” and battery life [8].

Therefore, a joining technique that is reliable with a narrow range of initial process parameter variation is required. Recently huge attention was given to laser welding (LW) as it is a very promising technique to enhance the safety and reliability of battery joints. Common materials for busbar and battery tab manufacturing are aluminum and copper. The laser welding process is a promising technique to join similar and dissimilar materials such as Al and Cu. The desired strength, ductility, fatigue life as well as electrical resistivity are crucial to attain in laser welding of dissimilar materials aluminum and copper in busbar to battery tab in BEVs. Laser welding machines use variable tools and techniques to shape laser beams, monitor the process in-line, and reach the high-quality joint. The laser welding process results in optimized power density distribution, and high feed rates combined with deep welds, while effectively preventing spatter formation and melt

ejections. Thus, higher efficiency and productivity than conventional techniques can be achieved in terms of energy consumption, wastage reduction, and production speed [19].

The current review paper mostly deals with laser welding of dissimilar materials aluminum to copper sheet in the busbar to battery tab joints. Also, the current review provides an adequate understating of the key factors influencing the Al–Al/Cu busbar to battery tabs joint properties as well as laser welding and laser brazing of similar and dissimilar Al–Al and Al–Cu sheet with potential application in battery joints of BEVs. A large part of the current review defines how the defects form such as IMCs and porosities during and after laser welding. The effect of materials properties in laser welding and laser brazing is discussed in detail. Laser-materials interaction during the laser welding process has been observed to strongly affect the defect formation and therefore the joint properties. Laser-materials interaction can be influenced by process parameters adjustment (e.g., laser power or speed), laser operational mode, and choice of materials (e.g., base metals, alloying elements, filler metals, etc.). The current combination of the above-mentioned items reduces the defects such as IMCs and hence enhances the joint properties in terms of mechanical and electrical properties.

2. Current joining technologies for EV batteries

A comparison of the common welding techniques for joining battery cells on a module level in BEVs can be found in the Table 1. Most of the techniques do not need filler metals or protection gases to make the joints, except for certain laser welding processes. Laser brazing and Laser welding will be discussed in detail. In addition to Ultrasonic welding, wire bonding can be performed by laser. Figure 1 shows a wire bonded battery joint.

Table 1. Assessment of current joining technologies in busbar to the battery terminal of battery electric vehicles (BEVs).

Joining technique	Pros	Con's
Ultrasonic welding	●Joining of similar and dissimilar materials (e.g., Al–Cu) ●Joining of multilayer Cu to Al plate [21] ●High level of productivity [22] ●Short welding time and low energy input [23,24] ●Suitable for pouch cells and prismatic cells [9]	●Electrical resistance increases with increasing the Al–Cu joint temperature [25] ●Misaligned welds lead to higher electrical resistance [26] ●IMCs formation [27] ●Inherent process vibrations cause damage to the battery [28] and previously welded joint [29] ●A tool condition monitoring is required ●The technology itself is challenging and not fully understood yet, due to its inherent multi-physical nature [8] ●Design limitation [9] ●Sensitive to surface roughness [24] ●Temperature rises to 660 ℃ during welding [30,31]

Continued on next page

Joining technique	Pros	Con's
Resistance welding [32]	●Low initial cost ●Welding of sheets ●Easy to automate ●Good quality control	●Thermal expansion and open cracks ●Hot cracking at elevated temperatures includes failure of the weld and cracking in the heat affected zone (HAZ) (liquation cracking) ●High-cost machinery ●Limited workpiece thickness ●Less efficient for high conductive materials
Wire bonding [33]	●Joining of dissimilar materials ●Easy automation ●No special monitoring is required ●Different techniques to create a wire bond e.g., laser welding ●Flexible design	●Limited to low joint strength and thin wire ●Special welding and clamping devices are required
Friction welding [34–36]	●Joining of Aluminum alloys ●Joining of copper (Cu) and aluminum (Al)	●Formation of IMC ●Formation of Kirkendall hole ●Design limitation for Al–Cu joints
Force fitting and mechanical assembly	●Comparable contact resistances compared to welded connections [37]	●Surface imperfection, contact pressure, joint type, and poor connection increase electrical contact resistance (ECR) and energy loss ●Generated heat at the interfaces [37–39]. ●Influence of vibrations on the electrical connection resistance [40]
Laser welding and laser brazing [41,42]	●High precision and productivity ●Low heat input and narrow HAZ ●Joining of similar and dissimilar materials ●A wide range of thicknesses ●Contact-free joining method ●Avoid thermal stresses ●Reduction of IMCs	●High capital requirements ●High power requirements ●Keyhole formation and instabilities in some cases

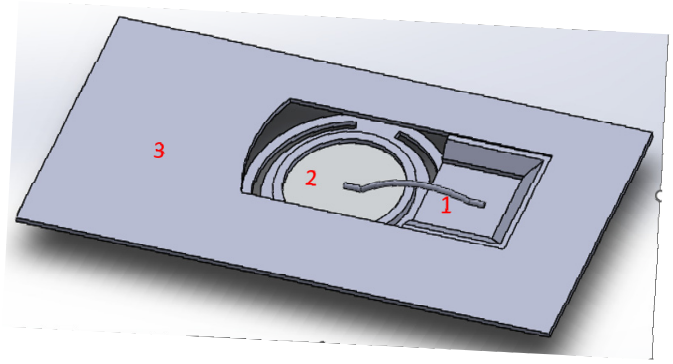

Figure 1. Wire bonded battery module connections; the no. 1, 2, 3 are respectively a wire, a battery tab, and a busbar [20].

3. Applications of dissimilar metal soldering and brazing and laser brazing

3.1. Brazing

To obtain the desired service condition, brazing controlling factors i.e., joint design, fillers metals, and process parameters should be properly defined. For example, to assure the desired mechanical properties in the case of dissimilar materials, the joint clearance, and thermal expansion coefficient must be taken into consideration. In the case of a high different thermal expansion coefficient, at least one of the components must endure deformation. In any case, some residual stress remains in the brazement which will be increased by stress during the service life. For example, in the case of brazing a ductile material (e.g., Ni-base alloys) to a base metal with a low ductility (that will undergo phase transformation at brazing temperatures such as carbides or heat-treatable materials), the joint should be designed in a way not to add to the stress during the service life. A good joint design distributes the stress in the base metal and prevents stress concentration from the edge of the joint (see Figure 2) [43]. The arrows show that by increasing the interface between the two parts from 1T to 4T and also a curved corner can lower the stress concentration in the braze joint.

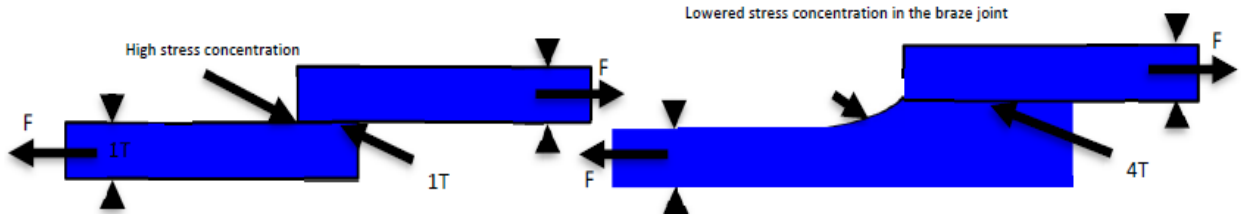

Figure 2. Shows lap joint design where there is high-stress concentration (left) and lowered stress concentration in the joint (right) [43].

Hayashi and Miyazawa [44] spot braze dissimilar material Al 1050 and oxygen-free Cu 1020 by a cover plate and a Cu–Ni–Sn–P brazing filler metal. The role of the cover plate was to transfer heat to base metals and prevent heat dissipation from those base plates. They have found out that using a Spill Prevention, Control, and Countermeasure cover plate (SPCC) on the copper side increased the joint strength by 40%. By increasing the brazing current (up to 1100 A) joint strength and ductility were increased. By increasing the current from 700 A to 1100 A, the location of fracture after the sheer tensile test moved from the joint to the Al side. In the case of brazing with 1100 A, a fracture happened on the aluminum side. Also, it is shown that increasing the brazing current leads to an increase in the brazing area, which can be interpreted as a reduction in the electrical resistivity of the joint [44].

Brand et al. [18,37] concluded that soldering gives the lowest connection resistance and highest tensile strength in comparison to laser, resistance, and ultrasonic welding as well as force-fitting in the case of joining a brass plate with varying connection areas to a 26650-battery cell format. Solchenbach, Plapper, & Cai [45] found a direct connection between the size of intermetallic compounds (IMCs) in the joint and the connection resistance. Brand et al. [46] and Solchenbach, Plapper & Cai [45] showed an inverse relationship between the joint area and joint resistance.

Sommer et al. [47] successfully performed brazing of thermally sprayed AlCuSi(Mg) Al plate to an Al fin in an industrial furnace at 540 ℃ for 3 min under a high vacuum of 8.7×10^{-4} mbar. They concluded that sound brazing of aluminum alloys is dependent on direct contact of joint partners, aluminum surface condition (surface oxide layer), Mg content, and brazing window. Magnesium content that is present either in filler metal or Al alloy (e.g., EN AW 3005) sublimes during the brazing and acts as a getter for oxygen and water vapor and inhibits oxide formation thus enhancing the brazing.

3.2. Laser brazing in busbar to battery tab

Laser brazing of aluminum alloys is growing rapidly in the automobile industry due to improved joint properties, cost efficiency, and productivity. In brazing, the base metals are not melted which means less heat input, less heat accumulation, and therefore less inner stress and deformation after the cooling process [48,49]. In the case of laser brazing of dissimilar materials, easier evaluation of laser brazed joints, shorter brazing period, limited IMC formation, and thus better mechanical properties are the advantages of laser brazing. Brazing of dissimilar materials with a substantial difference in thermophysical properties such as the coefficient of linear thermal expansion (CTE) may cause severe thermal stress and therefore residual stress may destroy the brazed joint during a fast-cooling rate [50]. However, the selection of a proper filler wire for bonding, and flux to remove the oxide layer and increase the surface wettability and heating efficiency were the subjects of investigation [48,49]. However, Markovits & Jászberényi [49] successfully laser brazed a 1050 Al plate to a 3005 Al tube using a CO_2 laser, and they observed a flame due to the burning of flux. Xiao & Dong [51] used a solid-state laser to braze-weld an aluminum plate to a copper plate with 3 mm thickness. They characterize α (Al) + Al_2Cu eutectic and Al_4Cu_9 intermetallic compounds at the interface. High power laser energy was employed to join the aluminum to copper. The excessive energy may lead to copper melting and the eutectic reaction and thus improvement of aluminum wettability on a copper surface [51,52].

Studies on brazing of Al to Cu with different filler wires [53,54] and laser brazing of Al–Cu with different alloying elements [55] indicate that the brittle IMCs at the interface of two metals can be substituted with phases showing higher mechanical properties.

4. Laser welding

Laser welding (LW) uses the heat of a concentrated beam of coherent, monochromatic light to create a fused weld. For a given joint geometry and material combination, the principal process variables are beam power, spot size, and welding speed. Two welding modes in the laser beam welding process are heat conduction welding and keyhole welding. The laser power density below 10^6 W·cm^{-2} allows welding in the conduction mode and like conventional fusion welding processes. In contrast, a power density in the range of $5 \times (10^6–10^7)$ W·cm^{-2} is sufficient to initiate local vaporization, and a narrow, deep vapor cavity, or keyhole, is formed by many internal reflections of the laser beam. The keyhole is encircled by a layer of molten material and is maintained by an equilibrium between vapor pressure, surface tension, and hydrostatic pressure. In this welding mode, a deep, narrow weld bead and heat-affected zone (HAZ) will be formed with fine microstructures, limited HAZ grain growth, beneficial non-equilibrium phases, and sometimes

detrimental phases such as IMCs (Intermetallic compounds) due to limited heat input and rapid cooling rate [56].

Welds can be produced at atmospheric pressure with the application of inert gas, such as helium or argon, to protect the weld bead from contamination, and suppress the formation of the plasma plume. Also, filler material in the form of a powder, intermediate plate, or wire can be introduced before or during processing [57–59]. The use of filler wire and inert gas is not currently widespread in the LW of battery joints. However, fillers may provide solutions to reduce the unwanted phases as well as mechanical and electrical properties improvement, some of which are described later [56].

Different lasers (e.g., fiber, Nd:YAG, diode) are available with a wide range of beam characteristics, wavelengths, and laser powers, with the possibility of pulse and/or continuous welding equipped with advanced techniques such as wobble welding techniques. In a standard LW, a collimated laser beam is focused to the desired spot size in a static path and a focal plane (for some examples look at Table 2). Wobble heads by incorporating scanning mirror technology move the beam and adjust the focal spot by changing the wobbling shape, amplitude, and frequency. More importantly, this technique enables laser welding of highly reflective materials, e.g., copper and aluminum, and enables new applications for e-mobility and specifically battery joining. Wobbling made it possible to use near-infrared (near-IR) wavelengths and reach tiny spot sizes and high-power density on the plate thus the need for frequency-doubled green lasers is not deemed. This feature forms a stable keyhole with a wide process parameter window leading to the formation of porosity and cracks free weld. With the advantage of altering weld width and depth needless of optic change or beam defocusing. For constant energy input, this technique allows tailoring the weld joint geometry, to generate a large weld contact area, which reduces resistance in the weld joint and provides a mechanically sound joint. In laser welding of busbar to battery tabs, it is common to see parts that have poor fit ups. The beam wobble technique has the potential to justify seam gap and offset. Wobble welding combined with wire feed may even bridge weld gaps as large as 1 mm in the case of welding 304 steel sheets [60].

In the case of laser welding of copper plate, in continuous-wave welding (CW) mode, increasing speeds above 10 m/min minimize the instabilities and stabilize the process. However, this means that the optimum weld process parameters are out of the range of conventional motion systems such as robots. As discussed before, by using wobbling and focusing laser spots down to 20 μm, a 1 kW single mode laser provides power densities as high as 1 MW/cm^2 and welding will be possible. In continuous-wave welding (CW), the laser coupling into the material will be once, however, in pulsed welding, this must happen for each pulse. Using the right combination of pulse profile, pulse energy and exposure time provides a high weld quality without defects such as blow holes or spatters at exceptionally low average power, which can be critical for welding heat-sensitive components, however, it may take longer production time than conventional laser welding. Using the long-pulse technique may alleviate this challenge by creating a quasi-continuous stable weld meaning the beam moves to a longer distance than conventional pulse welding during each pulse. In the case of foil laser welding of dissimilar materials using microsecond- to nanosecond-range pulses, provides the required pulse energy rapidly to produce high melt efficiency and stable welds [60].

Furthermore, integrated process monitoring technologies allow for collecting a range of valuable information in real-time during the welding process helping for defect-free laser welding in advanced industries. This may be emphasized even more when precise control over the weld-bead location and chemistry, and narrow fit-up tolerances are demanded. For example, using advanced

in-process monitoring technology such as Inline coherent imaging (ICI) can directly measure weld penetration and provide a wide range of valuable information in real-time and in any industrial production. ICI is based on interferometry, and adds a low-power, near-IR measurement beam to the existing laser head [60,61].

5. Applications of laser welding of Al–Al

Common defects in aluminum welding are hot tears in weld metal or heat-affected zone (HAZ), porosity, inclusion in the weld metal, lack of fusion, incomplete penetration, and softening in the HAZ. The formation of the above-mentioned defects depends on the metallurgical factors and welding process parameters. One of the main metallurgical concerns is the selection of proper filler metal. It should be chemically as similar as possible to the base metal mainly to avoid galvanic corrosion attack in an application. Also, filler alloys should be resistant to hot tears and provide enough strength and ductility. In the welding of low alloy aluminum alloys (e.g., 1XXX series), almost exclusively alloy Al1100 is used [62].

1xxx series (i.e., 1050, 1060, 1100) and 3003 aluminum alloys are common materials in busbar and battery tab applications. These alloys are non-heat-treatable groups of Al alloys that possess various features such as low density (about one-third of steel), high thermal and electrical conductivity, good combination of strength, ductility, and corrosion resistance, and readily laser weldability (See Tables 3 and 4 for physical and chemical compositions). These features make these Al alloys suitable for electrical connectors applications such as busbars and battery tabs in batteries. To reach a sound laser welded joint of aluminum alloys, some measures should be taken such as LW speed, key-hole instability, and fluctuation, shielding gas, laser power, and power density to avoid weak weld joint, porosity formation, HAZ degradation, hot cracking, and buckling during and after welding [63]. Kah et al. [64] stated porosities due to keyhole fluctuation/instabilities may form at the bottom, tip, or middle of the keyhole and they are usually of irregular shape and larger size than metallurgical porosities. In a study, Sun et al. [65] investigated the impact of focal position offset on joint properties of Al1050 to Al1050 in an overlap position using beam oscillation. The results of the investigation of weld geometry, thermal profile, weld porosity, and mechanical strength of the joint showed a reduction in the peak temperature and weld porosity due to the laser beam defocusing. However, defocusing more than 3 mm results in poor mechanical properties.

6. Principle of laser joining of dissimilar Al–Cu materials

Laser welding is a highly automated welding technique with a high-energy density beam, low heat input, high accuracy, and low spatter. Recently developed highly advanced laser welding machines can provide smooth welding with a spatter-free or almost spatter-free surface [66,67]. Laser welding is a well-established welding technique for aluminum to aluminum and copper to copper. However, in the case of welding dissimilar materials, e.g., copper to aluminum, the risk of IMC formation can cause difficulty. Additionally, the formation of hot and cold cracks and different thermophysical properties of the joint metals such as melting temperature and thermal conductivity may restrict the weldability [68]. Laser parameters adjustment [65,69–71], the addition of alloying elements, and the application of filler metals [58] are among the solutions to avoid IMC formation. The initial cost for installments and transportation of laser welding machines are high which makes

them suitable for a high number of production and a high number of repetitions. As laser welding is an overly sensitive technique, careful monitoring of the positioning of parts should be taken into consideration otherwise, the weld joint will be impaired [33].

Table 2 shows that much research was carried out in the field of laser welding of Al and Cu materials with thin thicknesses. These experiments are related to the laser welding of busbar to battery tabs. The shielding gas may alter the weld pool surface, the fluid flow, and hence metal mixing in the weld metal [72]. Nevertheless, it was shown in [73] that the influence of shielding gas on dissimilar Al–Cu welding is negligible. Most of the performed research did not use shielding gas [45,68,70,72,74–81].

As can be seen in Table 2, the literature survey shows fiber laser is frequently used in the welding of a sheet of dissimilar materials Al and Cu [45,58,67–72,74,76,82,84]. And laser welding were performed mostly in the lap joint configuration [70,72,80,82]. Standard methods for laser welding of battery connection are fillet joint, lap joint, and spot welds. For example, fillet joining may be used when there is a hole in the busbar.

Temperature monitoring is deemed to be necessary as the battery is sensitive to heat and therefore overexposure to heat cause damage to the battery. One example of temperature monitoring in laser welding by using an IR thermal camera, Scotch® Vinyl electrical tape**,** and FORMEX™ GK insulator can be seen in Figure 3a,b. The busbar is covered by 0.2 mm thick Scotch® Vinyl electrical tape to eliminate multi-reflections from the aluminum surface and a FORMEX™ GK insulator was placed behind the side busbar to avoid heat sinking. Three different probe lines were chosen to scan the temperature (see Figure 3c). As can be seen in Figure 3d, probe line 1 & probe line 2 showed temperatures above 120 ℃ for almost 4 s, and probe line 3 for 1.5 s. Therefore, it can be assumed that temperature rise during the laser welding process might not have significant effects on the battery [65]. Dimatteo et al. [69] using thermocouples in laser welding of submillimeter Al and Cu plates found out 10 mm from the welding area the temperature to be 45 ℃.

Table 2. The different research carried out in the field of laser welding of dissimilar materials Al–Cu in LW of busbar to battery tab.

Ref.	Material(s)	Thickness Al–Cu (mm)	Laser					Properties			IMC	Microstructure
			Type	P (KW)	Spot size (μm)	Joint type	Variable Laser parameters	Mech.	Elec.	Therm.		
[70]	Al 1050 H0–Cu1020 H0[a]	0.45–0.3	Nd:YAG		635	Lap	Pulse shape and distance	x	x	x		x
[65]	Al 1050 H11–Al 1050 H14	1.5–2	Diode		268	Lap	●Focal position offset ●Beam oscillation frequency	x		x		x
[82]	Al 1050 H14–SF–Cu H14	0.21–0.2	Fiber	0.4	31	Lap			x	x	x	SEM, XRD
[68]	Al99.5–Cu99.5OF	1–1	Fiber	2	20	Lap Butt	●Beam oscillation mode (1D & 2D) ●Scanning width ●Lateral beam displacement	x			x	OM, SEM, EDS
[83]	Al 1050–Cu99.95OF[b]	0.6–0.6	Disk	0.95–1.8	89	Lap	●Laser power ●Oscillation amplitude	x			x	x
[72]	Al 1100–Cu (C10100)	0.2–0.5	Fiber		115	Lap	●Laser power ●Welding speed			x	x	EDS
[81]	Al 1050–SF Cu	0.21–0.2	Fiber	0.4	31	Lap					x	OM, SEM, EDS,
[74]	Al 1050–SF Cu	0.2–0.5	Fiber			Lap	Pulse time	x	x		x	x
[80]	Al 99.5–Cu 99.99	0.6–0.6 1–1	Solid-state		89	Lap	●Laser power (CW) ●Wobbling		x		x	OM
[79]	Al 1050–OF Cu 99.95[b]	0.4–0.4		1.1	89	Lap	Pulse profile/shape	x			x	x
[69]	Al 1050–C1020–HO Cu[a,c]	0.45–0.3	Fiber	1	60	Lap	●Laser power ●Welding speed ●Wobbling amplitude	x	x	x		x
[84]	Al3003 H14–Cu110–H00	0.49–0.54	Fiber	0.5	10	Lap		x				OM, SEM, EDS
[85]	Cu–Cu	0.3–0.3	Fiber	0.4	25	Lap		x				

Continued on next page

Ref.	Material(s)	Thickness Al–Cu	Laser					Properties			IMC	Microstructure
			Type	P	Spot size	Joint type	Variable Laser	Mech.	Elec.	Therm.		
[86]	Al 1050–Cu[(c)]	0.3–0.3	Fiber	1	20	Lap	Welding speed	x			x	SEM, EDS, XRD
[75]	Al 1050–Cu	2-2	Fiber	2		Butt	Laser beam off-set		x			x

[(a)]Ni plated copper with a thickness of 2.5 µm

[(b)]Welding from the Cu side

[(c)]Both Al–Cu and Cu–Al configurations

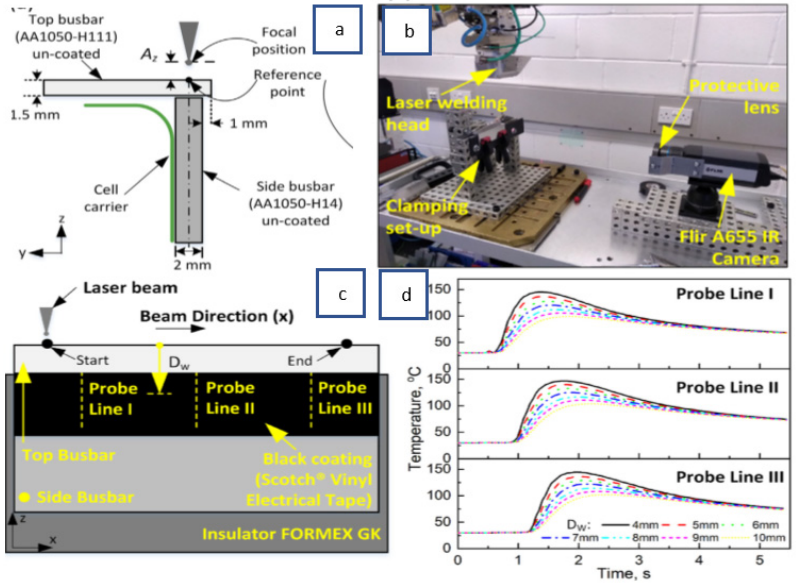

Figure 3. Temperature monitoring: (a,b) welding set-up, (c) probe lines, (d) the results of temperature monitoring [65].

7. Effect of materials properties on laser joining

7.1. Physical and chemical properties of the base materials

Aluminum 1xxx series (>99% Al) and aluminum 3003 are non-heat-treatable groups of Al alloys that possesses various features such as low density (about one-third of steel), a good combination of strength and ductility, corrosion resistance, thermally and electrically conductivity, and readily laser weldability. These features make these Al alloys suitable for electrical connectors applications such as busbars and battery tabs in batteries. Pure Copper plates with different purity grades such as 99.9% (electrolytic) and 99.995% (oxygen-free high-conductivity) or Ni-plated pure copper with thicknesses in the range of a few hundred micrometers up to a few millimeters were used in the experiments. It has been shown that joining Ni-plated copper busbars significantly improves the metallurgical and contact properties [87–89]. The chemical and mechanical properties of common materials in busbar and battery applications can be found in Tables 3 and 4.

Table 3. Common Al and Cu alloys in laser welding of busbar to battery tabs.

Alloy designation	Yield	Tensile strength	Elongation in	Thermal conductivity	Electrical resistivity
AA 1050-H14 [90]	85	105–145	2–6	222	2.8×10^{-8}
AA 1100-O [91]	20–34.5	75–105	15–28	222	2.99×10^{-8}
AA 3003-O [90]	35	95–135	15–24	231	3.4×10^{-8}
Annealed Cu (C11000)	69	220	45	388	1.7×10^{-8}

Table 4. Chemical composition (WT%) of common aluminum alloy for busbar and battery tabs [92].

Alloy designation	Si	Fe	Cu	Mn	Mg	Cr	Ni	Zn	Ti	V	Others[a]		Al min.
											Each	Total[b]	
EN AW-1050	0.25	0.40	0.05	0.05	0.05	-	-	0.07	0.05	-	0.03	-	99.50[c]
EN AW-1060	0.25	0.35	0.05	0.03	0.03	-	-	0.05	0.03	0.05	0.03	-	99.60[c]
EN AW-1100	0.95 (Si + Fe)		0.05–0.20	0.05	-	-	-	0.10	-	-	0.05	0.15	99.00[c]
EN AW-3003	0.6	0.7	0.05–0.20	1.0–1.5	-	-	-	0.10	-	-	0.05	0.15	Bal.

[(a)]"Others" includes listed elements for which no specific limit is shown.

[(b)]The sum of those "Others" metallic elements 0.010% or more each, expressed to the second decimal place before determining the sum.

[(c)]The aluminium content for unalloyed aluminium not made by a refining process is the difference between 100.00% and the sum of all other metallic elements present in amounts of 0.010% or more each, expressed to the second decimal place before determining the sum.

7.2. Materials and potential defects

The high reflectivity and high thermal conductivity of aluminum and copper alloys may present some problems regarding keyhole initiation and maintenance. In laser welding of Al to Cu plate, Hailat et al. [84] observed only porosities in the Al part. In the case of laser welding of aluminum alloys, porosity is a frequent problem in partial penetration. In the case of keyhole mode, the

complex nature of the keyhole, keyhole instabilities, keyhole fluctuation, and high solidification rate also leads to porosities. Porosity can also originate from the volatilization of magnesium and zinc in the case of some aluminum alloys. As well as porosities due to fluid flow dynamics in the weld pool and hydrogen rejection in the solid-state, which is a common defect, as is solidification cracking in certain alloys. Also, Schmalen and Plapper [93] explained that hot cracks and pores can be the result of irregular gas shielding and the turbulent flow of the molten aluminum fluid. HAZ degradation in laser welding of Al to Cu may happen on the Al side which may lead to highly localized mechanical property variation and eventually failure at service [64].

Intermetallic compounds typically form due to the Al and Cu intermixture during laser welding. A significant difference between the physical properties of aluminum and copper results in brittle intermetallic structures and poses problems in weld metal formation [94]. IMC growth may happen due to the interdiffusion of Al and Cu in the interface of the Al–Cu joint during charging and discharging in a long-term application. The Al–Cu intermetallic compounds behave highly resistive when exceeding a distinctive limit of 3–6 μm [45]. However, Furuya et al. [55] using Ni alloying element led to a higher thickness of IMCs layer, but slightly thicker reaction layer therefore, it results in a similar electric resistivity and enhanced mechanical properties in comparison to laser welding of Al and Cu. Common intermetallic of Al and Cu (see Table 5) was observed to be formed during laser welding and in long-term battery application [72,82]. Also, some other IMCs can be seen due to the application of filler wires or metallic interlayers such as Cu_6Sn_5 and Cu_3Sn [95], and TiAl [96]. Other typical weld imperfections in laser welding are lack of penetration, root notches, undercuts, and lack of fusions.

Table 5. Observed intermetallic phases in the interface of the Al–Cu laser welded joints [82].

Phases	Composition (at% Cu)	Specific electrical resistance (μΩ·cm)	Hardness
γ_2, Al_4Cu_9	62.5–69.0	14.2–17.3	549
ζ_2, Al_3Cu_4	55.2–56.3	12.2	616
η_2, AlCu	49.8–52.3	11.4	628
θ, Al_2Cu	31.9–33.0	7.0–8.0	324

7.3. Effect of thermal expansion

A significant difference in thermal expansion is challenging when it comes to laser welding of dissimilar materials, as it results in high residual thermomechanical stresses in the joint and therefore a weak joint with cracks which may result in failure [97]. After the joint formation, temperature increase results in the lateral movement of Al plate more than copper in the contact zone, shearing the contact area and therefore reducing the contact area, which increases the joint resistance and thus temperature rise at the connection. Also, with the repetition of the heating and cooling cycle, thermal stresses may build up considerable plastic deformation in the contact zone which accelerates the degradation of the connection [98].

7.4. Laser absorptivity as a function of surface roughness

ASM Handbook [42] explains that energy absorption or reflection by a target is a function of laser wavelength and surface emissivity of the target. More recently, Helm et al. [85] showed that

surface properties of the connector materials in battery cells increase the laser absorptivity nevertheless not improving the mechanical properties. However, Kaplan [99] discussed that the material temperature is the main factor for absorption, during the process. While Huntington and Eagar concluded that joint geometry and the surface condition have the main roles [100]. And the laser absorptivity in keyhole mode will be influenced only by the surface condition in the initial stage when the surface is heating up to saturation [100,101].

8. Laser-Matter interaction and the resulting joint characteristics in terms of IMCs formation, mechanical and electrical properties

8.1. Role of welding speed

One issue with copper welding at low speed is the spatter formation and blowholes due to the low viscosity and surface tension of the melt. Increasing laser welding speed above 10 m/s may solve the problem, however, the depth decreases, and the weld bead will be narrow. In other words, a decrease in welding speed leads to an increase in the heat input and therefore a wider and deeper weld [60]. With a fixed heat input, the molten pool dimensions have also an inverse relation with the welding speed, as shown in Figure 4. Figure 4 shows with the heat input fixed, the molten pool dimensions slightly decrease from Figure 4a-1 (i.e., low laser power and welding speed) to Figure 4a-3 (i.e., high laser power and welding speed). This can be justified by the fact that the available time for heat to stay in the sample is shorter for the case at the bottom due to higher laser welding speed, therefore a smaller portion of the absorbed laser power will be utilized to form a molten pool locally. Also, a different mixing pattern can be seen in the three different cases with the same heat input. Case 1 (i.e., lower laser speed and power) showed an even mixing while case 2 (i.e., higher laser speed and power) resulted in a vortex mixing pattern [72].

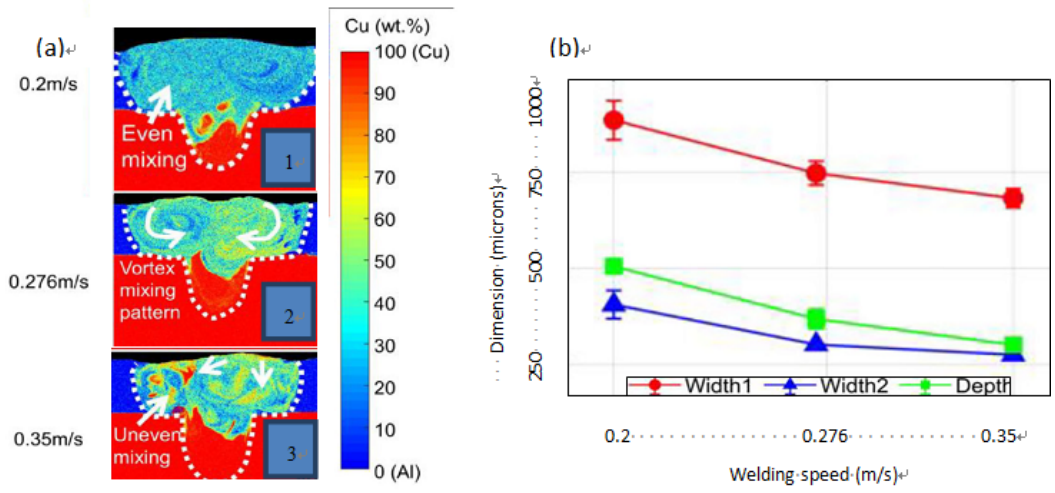

Figure 4. EDS image of the molten pool geometry (white dashed curve), Cu concentration field, and mixing pattern (left image) and effects of welding speed on weld joint geometry (right image) in a fixed heat input [72].

8.2. Role of welding power/energy

In general, at the same welding speed, increasing power increases weld pool dimension and a higher level of intermixture and thus higher levels of IMCs formation and likely cracks due to the formation of IMCs such as Al_2Cu, AlCu, Al_3Cu_4, and Al_4Cu_9 layers [72]. In the case of laser welding of Al to Cu, from the Al side, Schmalen and Plapper [74] explained the relationship between the electrical resistance and mechanical properties. The laser power may affect the mechanical properties and electrical properties (i.e., electrical resistance) of the joint by changing the degree of intermixture and IMC layers thicknesses and their distribution. In the case of keyhole welding, increasing the power leads to the fabrication of a proper joint with good mechanical and electrical properties because of the limited thickness of the IMCs layer (i.e., 3–6 μm). After this point, increasing power, increases intermixture between copper and aluminum, growth of IMCs layers, an increase in the hardness thus an increase in el. Resistance, reduction in ductility and overall degradation of mechanical properties [74,80] (See Figure 5).

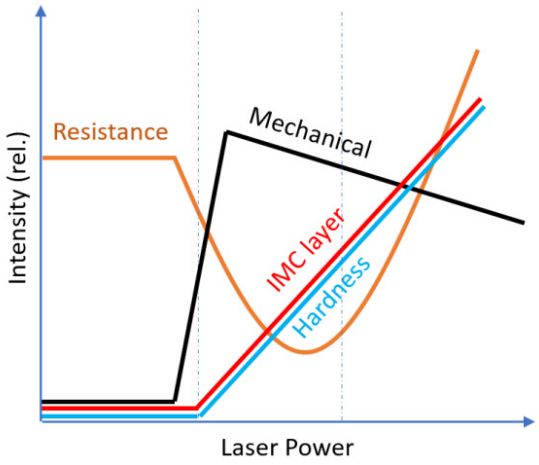

Figure 5. Al–Cu joint properties in terms of electrical resistance, mechanical properties, IMC layer, and hardness [80].

8.3. Laser power modulation

The output power of a laser (e.g., fiber [102], solid-state [103], or diode [104]) can be modulated by changing the signal input/driving current, or by alternating the continuous wave output. Alteration of the current or voltage with time may modulate the output signal. Direct Modulation is when the current, before reaching the laser diode, is modified with the desired signal for the application. External Modulation is when the modulation is imposed onto the laser signal after the light is generated. External modulations such as Electro-Optic Modulation (EOM), Acousto-Optic Modulation (AOM), and Electro-Absorption Modulation (EAM) manipulate the output with electric fields or sound waves. Both types of laser power modulation are shown for a diode laser in Figure 6 [105,106]. Application of laser power modulation with proper parameters may stabilize the welding of copper, welding of aluminum, thus minimize weld defects and improve the weld quality (See Figure 7).

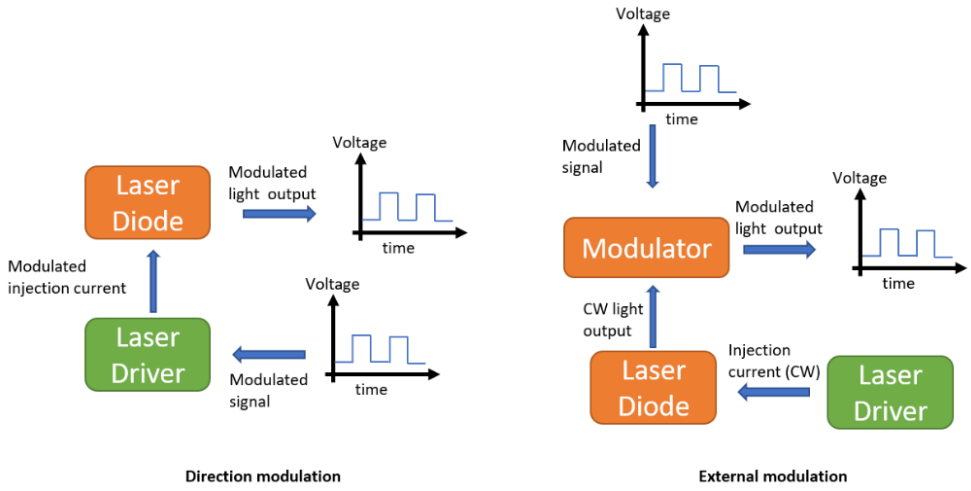

Figure 6. Direct modulation and external modulation. This figure is adapted from [105,106].

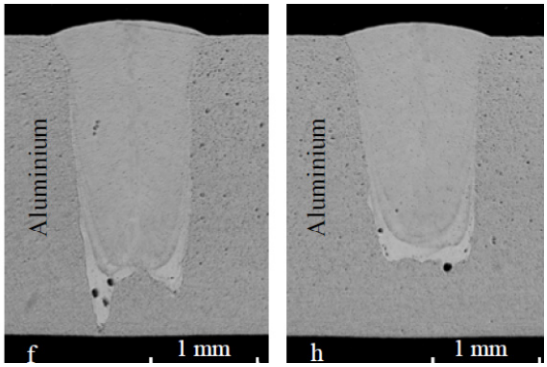

Figure 7. Left and right images are without and with laser power modulation, respectively [68].

8.4. Pulse laser welding

Schiry and Plapper [107] employed a 400 W fiber laser with pulse times between 24 and 48 μs to weld Al to Cu welds in an overlap configuration in the same circular beam movement as shown in Figure 8. The results showed that the formation of IMC correlates with the pulse time i.e., longer pulse time leads to a higher intermixture of Cu and Al and increased formation of IMC. The optimum electric resistance was achieved with a pulse duration of 24 μs meaning a complete bonding and a low amount of IMC. A pulse time of 18 μs results in poor pulling strength and toughness. A slight increase of the pulse time up to 21 μs enhances the strength greatly. A longer pulse time (i.e., 36 μs) leads to a brittle joint [107].

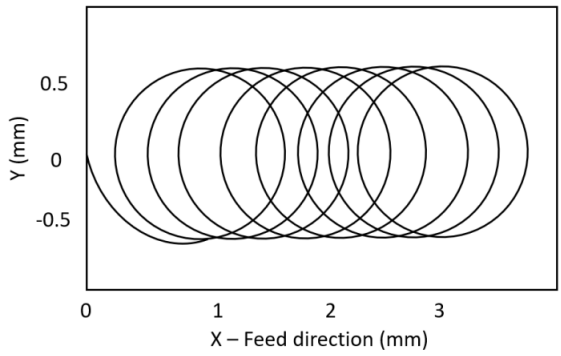

Figure 8. Beam circular movement [93].

Lerra et al. [70] investigated the effect of pulse shape and distance on dissimilar laser welding of Al and Cu. The pulse distance can be defined as the distance between the initial points of two consecutive pulse. Also, pulse distance (d) and frequency (f) can define the circular welding speed Vc = f × d (see Figure 9). Table 6 shows the applied laser parameters in the experiments. Figure 10 shows the effect of pulse distance on seam morphology. In the case of D and E in Figure 10 the bonding was inefficient. Also, they found out that the ramping up pulse shape (i.e., using pre-heating) gained higher strength than their counterparts those are, decreasing step pulse shape and decreasing ramp pulse shape (see Figure 11).

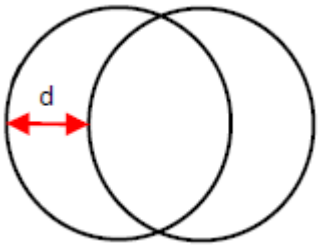

Figure 9. Pulse distance representation.

Table 6. Experiment configuration of Al–Cu Laser welding. Reproduced from Ref. [70] with the permission.

Peak power (KW)	Pulse energy (J)	Pulse frequency	Welding speed (mm/s)	Pulse distance (d) (mm)
6	8–23	9–24	1–29	0.1, 0.32, 0.55, 0.8, 1.2

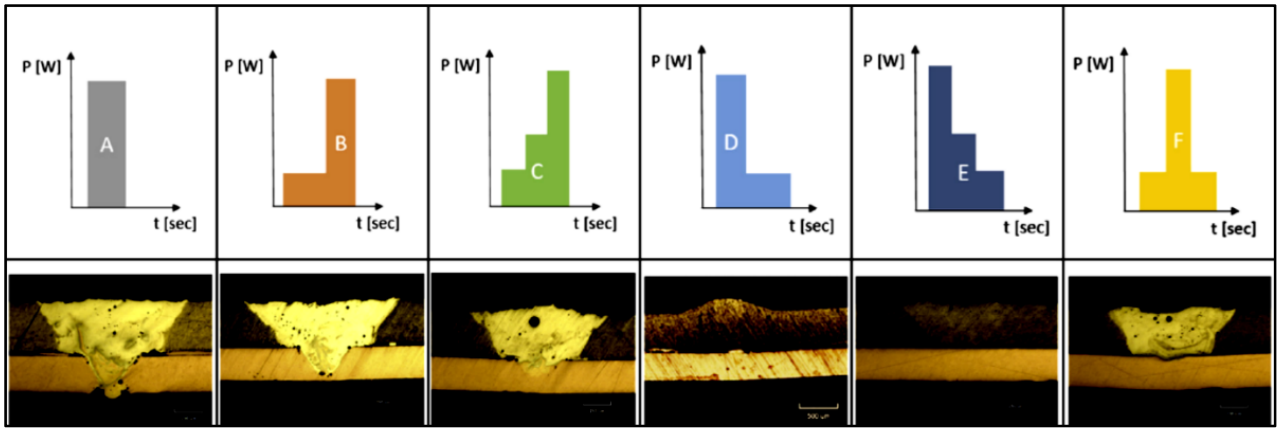

Figure 10. The effect of pulse shape on the seam morphology with E = 13 J and d = 0.32 mm for various pulse shapes: (a) square pulse, (b) increasing step pulse, (c) increasing ramp pulse, (d) decreasing step pulse, (e) decreasing ramp pulse, (f) central peak pulse. Reproduced from Ref. [70] with the permission.

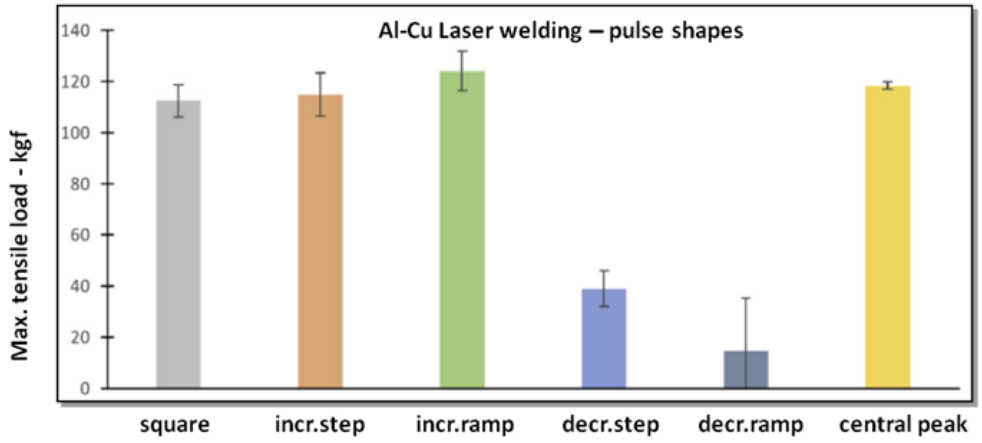

Figure 11. The effect of pulse shape on the max. tensile loads. All tests were performed with a pulse energy of 13 J and pulse distance of 0.32 mm. Reproduced from Ref. [70] with the permission.

In the case of square pulse shape (or the standard shape) the pulse distance and maximum tensile load correlate with each other very well. By increasing the pulse distance up to 0.55 mm, the tensile strength increases the highest as well as displacement in the joint, and after that, the tensile strength starts to reduce gradually. In the case of pulse shape and pulse distance of 0.1 mm, the joint is highly brittle due to the elevated level of intermixture. It is probably due to a higher number of IMCs as the hardness shows (see Figure 12). The decreasing step pulse shape and decreasing ramp pulse shape showed the highest electrical resistance (K factor) due to inefficient joints. In the case of a square pulse, the lowest K factor (i.e., 1) which is similar to the Al base metal, and the maximum tensile load (120 kgf) happen simultaneously (see Figure 13).

The effect of pulse modulation by alteration of pulse time was studied by Mathivanan and Plapper [79]. The laser oscillation in the form of infinite shape on Al-Cu joints with a fixed laser

pulse energy of 4.02 J, peak power of 1100 W, a pulse width of 5 ms, and frequency of 150 Hz was used. The results showed that by increasing the active welding energy, the metals interdiffusion and defects like pores and cracks increase although the same energy was delivered in all conditions. Laser pulse profiles with a pre-heating step (i.e., ramping-up energy) showed higher joint strength than their counterparts. This fact has been observed in a study by [70]. Pulse profile with pre-heating step (i.e., ramping up energy), proper active welding time, and effective cooling leads to a proper joint. In this case, the fracture was ductile and far from the joint on the Al side and probably in the HAZ of Al. [74] also investigated the effect of pulse shape on the joint properties in terms of hardness, pulling force, toughness, and electrical properties. The experiment was performed on 0.2 mm Al 1050 to 0.5 mm Cu with a focal diameter of 33 µm. They found out that a process window (pulse time (i.e., pulse width) of 21 to 30 µs) results in process robustness. Increasing pulse time to more than 36 µm results in high intermixture and high electrical resistance and a brittle joint. In one microscopic observation they reported existence of four different IMCs layer (i.e., γ Al_4Cu_9, ζ Al_3Cu_4, η AlCu, θ Al_2Cu) with a thickness of 20 µm [74].

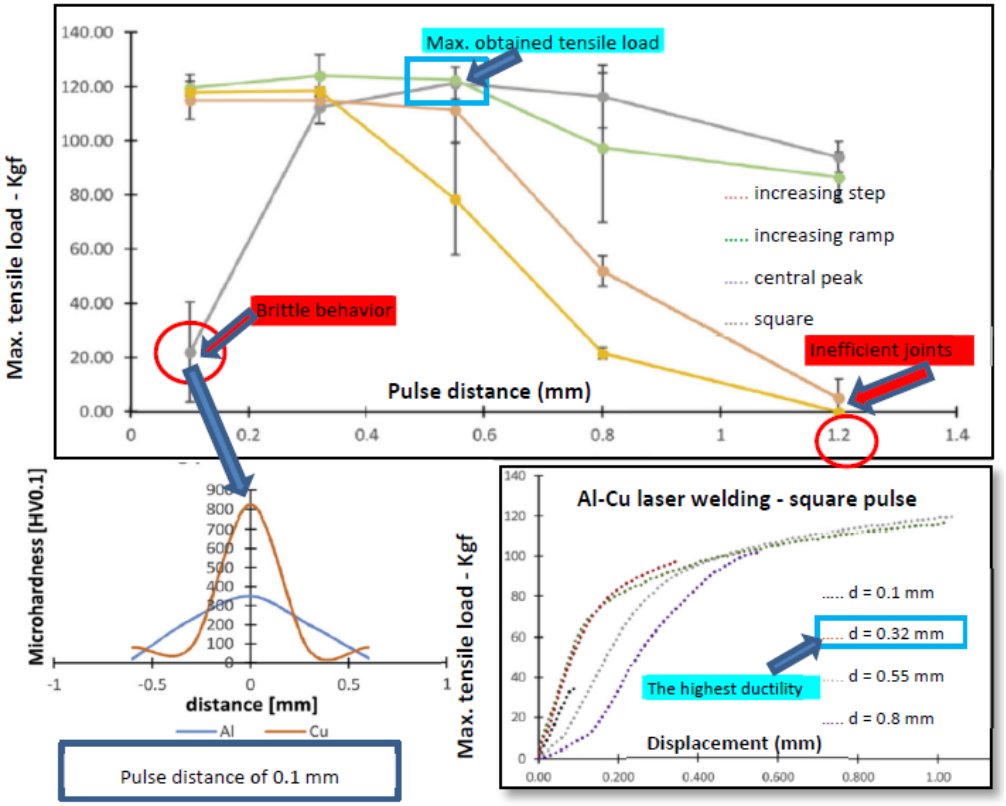

Figure 12. Shows bonding strength vs. pulse distance. The pulse shape using pre-heating gained higher strength than their counterparts. In the case of square pulse shape (or the standard shape) the pulse distance and max. Tensile load corresponds to each other very well. Reproduced from Ref. [70] with the permission.

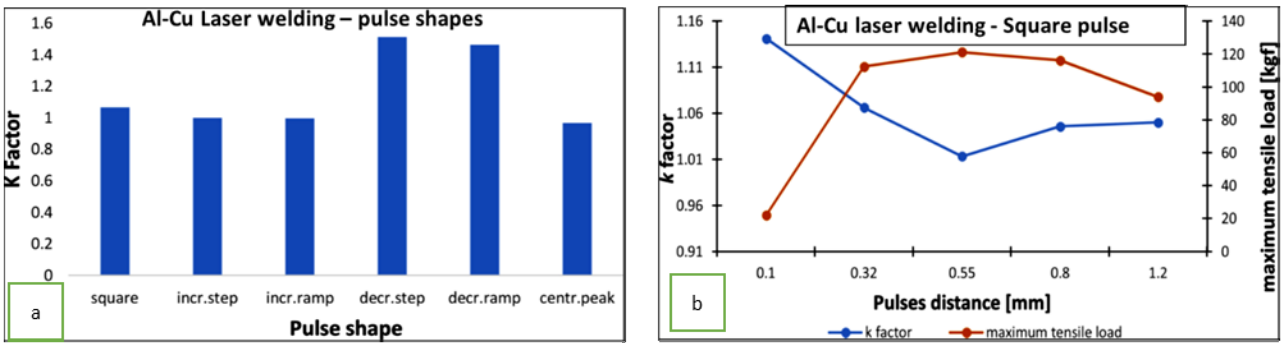

Figure 13. Demonstrates the relationship between the k factor (electrical resistivity) and pulse distance for different pulse shapes (a) and square pulses (b). Reproduced from Ref. [70] with the permission.

8.5. Beam oscillation or wobbling

Welding with oscillating laser beams enables adjustment of the bonding geometry. One or two-dimensional laser beam oscillation is applied for gap bridging during fillet welding in lap joints. The oscillation parameters are adapted to the gap size, in order to generate sufficient molten material and melt pool width, or to influence melt pool dynamics, e.g., for better degassing [108]. Kraetzsch et al. [68], using the oscillation frequency in 1-D scanning mode showed that increasing the scan width may result in a homogeneously mixed weld zone but with a higher level of porosity. They have also reported that the lateral laser beam dislocation in the joining area leads to different levels of materials intermixture.

Schmalen et al. [81] used Trumpf Trudisk2000 and 2D scanner of PFO 20 (focal length collimator = 90 mm, focal length optic = 160 mm, focal spot diameter = 89 μm) in CW mode with 600 W power output and 0.25 mm spatial beam oscillation and no shielding gas. The experiment was purposefully designed in a way to reach thick IMCs layers and large cracks. Four major IMCs namely θ phase (Al_2Cu), η_2 (AlCu), δ-phase (Al_4Cu_9), γ_1 phase (Al_4Cu_9) have been identified from etched micrographs and confirmed by EDS analysis and μXRD. Also, tts-μXRD revealed the presence of ζ_2-phase (Al_3Cu_4). The cracks propagate near the Cu side and through the interface between η_2 and γ_1, as can be seen in Figure 14. It was found that cracks propagate in a region between Al_2Cu and Al_4Cu_9, and commonly between Al_3Cu_4 and Al_2Cu_3. Solchenbach et al. [82] also found the fracture between Al_3Cu_4 and Al_2Cu_3 after electro-aging a laser-welded joint for 24 h, where Cu was electro positively charged.

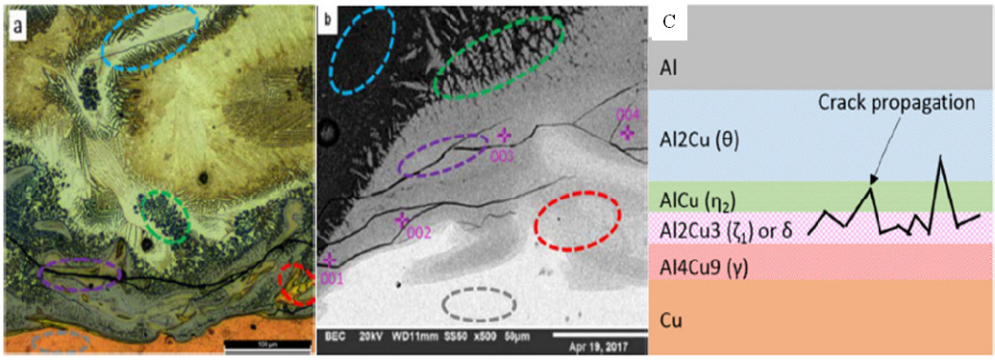

Figure 14. Shows that cracks propagate near the Cu side and through the interface between η_2 and γ. The circles show the same locations (a) Etched cross-section of Al–Cu joint, (b) SEM image of the weld joint (c) Schematic illustration of crack propagation [81].

Schmalen and Plapper [80] showed in a study where Al 99.5% and Cu 99.9% in overlap position were joined by laser-welding. The size of the sample is 40 × 45 mm with a 10 mm overlap. The thicknesses of the welded samples are 0.6 mm Al-0.6 mm Al, 1 mm Al-1 mm Cu, and 1.5 mm Al to 0.4 mm Cu. In the process initiation, increasing the laser power decreases the electrical resistance up to the formation of a proper weld. Then, the thickness of the IMC layer increases, and therefore resistance increases but not at a constant rate. Increasing laser power in both modes (i.e., welding with or without wobbling) showed higher electrical resistance than Cu plate. However, LW with wobbling showed a higher increase indicating a different behavior in the growth rate of the IMCs layer [80].

Laser welding of Al to Cu with a configuration where Cu is located at the top was rarely studied [83,109]. The effects of laser power and beam oscillation width for a copper-aluminum where Cu was located on the top were investigated by Mathivanan and Plapper [83] (see the configuration in Figure 15). High laser power and oscillation were intentionally utilized to overcome the laser reflectivity of copper and to form a vigorous mixing of fusion zone. Mathivanan and Plapper [83] showed by proper selection of wobbling form and amplitude and accordingly laser power a joint with nearly the same mechanical properties can be achieved as where the Al plate was located at the top. Large oscillation with the same laser power increases the weld zone and decreases the weld penetration. Increasing the wobbling amplitude demands higher power to form a large and vigorous mixing of the base metals. However, it should be considered that continuing to a higher power may lead to a reduction in shear strength due to the formation of detrimental phases. It can be concluded that the laser power modification according to wobbling pattern and amplitude may act as an important factor in the laser welding of dissimilar materials Al–Cu. Also in this experiment, three different modes of fracture based on the location of the failure and shear force are shown in Figure 16. In the first case, the weld seam development was very thin, and the entire seam undergoes the shear force. Crack propagation is along with the interface (horizontal) of the Cu–Al joint. The type of failure is brittle, and it happened at the interface of the Al–Cu joint at the IMC layer. However, they did not discuss the role of IMC in the failure mechanism. Ductile fracture happened away from the fusion zone and on the Al side, with significant deformation. A combination of a remarkably high intermixture region (including brittle phases) with a low intermixture region (including mechanical

microinterlocking at the interface i.e., “saw tooth interface” and “piercing of copper melt into the aluminum side” are thought to be the reasons for high strength of the laser-welded joint. And the third failure mode is a failure in the fusion zone i.e., separation at the edge, or the weld centerline. The different intermixture caused by the beam oscillation produces a discontinuous fusion zone with altering depth in a cross-sectional direction [83].

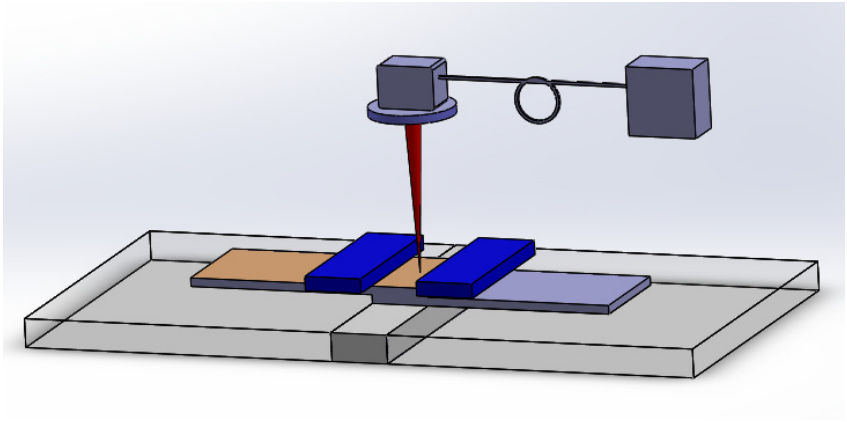

Figure 15. Sketch of laser welding setup for a configuration where the copper plate is located on top [83].

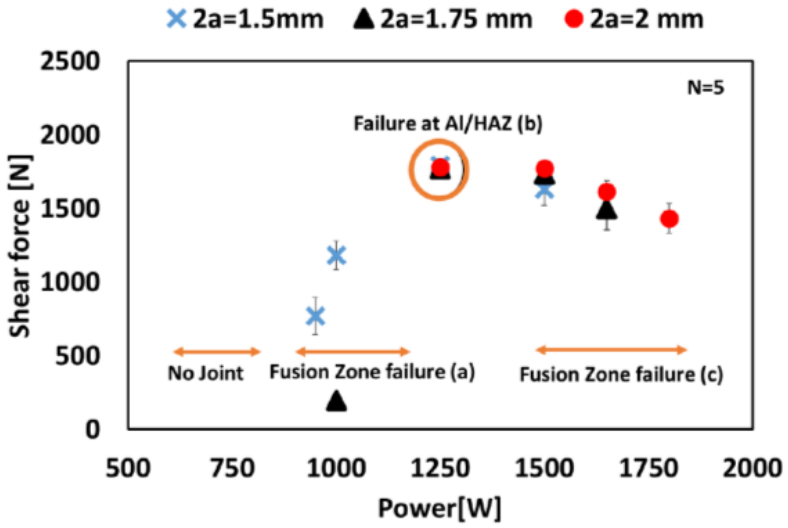

Figure 16. Shear strength (in Newton) for Cu–Al joints (copper on top for different power and oscillation widths of 1.5, 1.75, and 2 mm [83].

The Wobbling is not limited to CW lasers, and it can be applied to pulsed lasers such as millisecond quasi-CW fiber lasers. This feature allows welding of Al to Cu with high weld quality and exceptionally low average power which is critical for heat-sensitive applications [60]. The laser beam oscillation can bridge gaps for a weld material and welding setup without adjustment of laser power and speed. In addition, using laser beam oscillation, process emissions such as spatter and melt ejections can be reduced [110,111].

A single and multimode fiber laser with a small spot size and high-power density can be used to

weld materials such as aluminum and copper in battery production. The combination of high-power density and beam oscillation can overcome the challenges of the high reflectivity and high heat conductivity of highly reflective materials. Also, it can create a stable keyhole with minimum impact on penetration depth thus avoiding pores, and other defects such as weld cracking at low linear welding speeds. Figure 17 illustrates the effect of varying wobble amplitude at 400 W laser power and a 200 µm spot on SS304 material, showing how welds can transition from keyhole- to conduction mode. Also, it can be concluded that the different wobbling patterns (see Figure 18) does not significantly change the weld bead geometry [60].

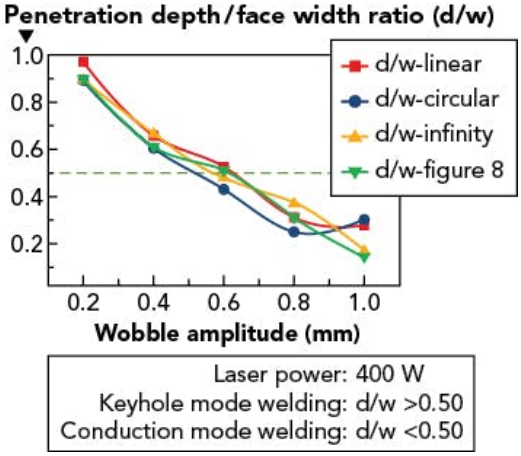

Figure 17. Illustrates the effect of varying wobble amplitude at 400 W power and a 200 µm spot on SS304 material [60].

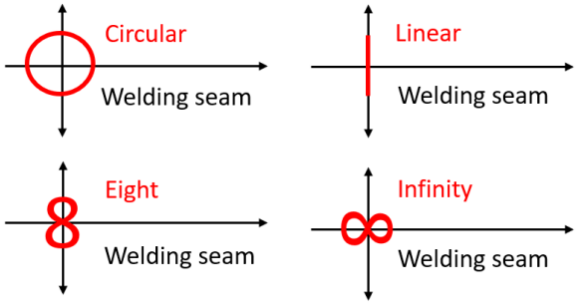

Figure 18. Laser oscillation pattern [60].

In the case of joining dissimilar materials such as aluminum and copper, in addition to their different thermophysical properties, their weldability is limited by the formation of coarse brittle intermetallic phases and the formation of hot and cold cracks [68]. By using optimal oscillation parameters, the metallurgical formation of these intermetallic phases in the weld can be specifically controlled and weld defects can be minimized. This enables to achieve strong welds with the required electrical and thermal conductivity.

Dimatteo et al. [112] laser-welded two pure copper sheets (i.e., 0.35 mm thick, 45 mm wide, and 60 mm length) with a thin layer of electroplated nickel (2.5 µm) to two pure aluminum sheets, i.e., EN-AW 1050 (0.45 mm thick, 45 mm wide, and 60 mm length) in a lap-joint configuration

utilizing fiber laser with a wavelength of 1070 nm. The weld seam with a length of 40 mm and an overlap of 10 mm was performed with a varying cycloid oscillation amplitude. The results showed that with the same laser parameters, as the wobbling amplitude increases the penetration depth and interface width decrease due to the larger scanning path and less heat concentration. The same scanning amplitude and increase in energy density led to a linear decrease in the maximum breaking load. While at the same energy density, increasing wobbling amplitude slightly reduces the maximum breaking loads due to the need for excessive heat and thermal cycles which favored the appearance of IMCs and resulted in a fragile fracture. At a wobbling amplitude of 0.2 mm with an energy density of 0.0225 MJ/cm^2, the optimum maximum breaking loads were reported to be 1010 N confirmed by a ductile fracture. When wobbling amplitude was set at 0.2 mm, EDS analysis showed θ (Al_2Cu) phase with the shape of serrated and Al–Cu eutectic alloys with vermicular shape. With 0.4 mm wobbling amplitude, η (AlCu) phases in the form of columnar grain can be seen as well as thicker IMCs layers. It can be concluded that the lower wobbling amplitude leads to limited intermixture, limited IMCs formation at the interface, and therefore the lower values of electrical contact resistance and higher values of mechanical properties [112].

8.6. Role of surface condition

Removing the oxide layer from a material surface is important to ensure a reliable joint strength in the joining of some dissimilar materials [113], though this is not always the case. For example, Schmalen et al. [73] showed that the cleanliness of the surface and surface precondition (i.e., laser-ablated surface, and surface sanded with corundum) has a negligible effect on the quality of laser welded joints. However, in many studies, the surface was cleaned with acetone before welding. Even Helm et al. [85] showed that surface properties (i.e., surface oxidation as well as surface roughening) of the connector materials in battery joints reduce the mechanical properties of the welded joints. They identified brittle oxide in the joint area as a possible cause for reduced mechanical properties. Regardless of insignificant mechanical properties alteration of the joint, it remained a puzzle how surface conditions may affect the electrical properties of the joints.

8.7. Filler metals

According to Schmidt et al. [114], laser beam can ideally produce a joint with nearly no electrical resistance since this technique allows arbitrary weld seams. In some cases, Al is replacing Cu to reduce weight and cost in the electrical components. There is a high affinity between Al and Cu to form intermetallic. These intermetallic compounds (IMC) weaken the mechanical properties of the joint. Some methods to decrease the IMC formation such as laser brazing [45,51,115], arc brazing [53,116], and solid-state welding [36,117] were tried. However, it is not enough to reach a thin layer of IMCs since the thickness of the IMC layer in the joint grows in application due to the Joules effect [55]. Therefore, another solution should be taken into consideration.

Esser et al. [118] and Mys and Schmdit [96] reported the formation of a ductile ternary alloy due to the application of a filler material that has a metallurgical affinity to aluminum and copper base metals such as nickel, silver, and tin. These alloys are able to enhance the mechanical properties of the joint. Also, some other investigations show that the addition of alloying elements to the Al/Cu joint can enhance the mechanical properties of the joint e.g., application of Al–Si and Al–Cu–Zn

filler wires, as well as Ni and Sn foil (SnAgTi) [53–55,84]. It has been discussed that increases in the thickness of the IMC layer degrade mechanical and electrical properties [45]. Furuya et al. [55] showed by the addition of Ni interlayer and therewith formation of (Cu, Ni) Al intermetallic layer between the weakest IMCs interfaces, i.e., θ-Al_2Cu and γ_1-Al_4Cu_9 enhanced the mechanical properties (see Figure 19). This investigation indicates that not only IMC thickness reduction, but the microstructure of the IMC layer also alters the joint's properties. (Al, Ni) and (Al, Cu) IMCs have similar electrical resistivity therefore, the effect of (Al, Ni) intermetallic in electrical resistivity is negligible. Also, it should be noted that Tavassoli et al. [119] reported that the electrical resistance of the Al–Cu joint depends on the total thickness of the reaction layer rather than the IMCs layer alone. And in this case, even though the addition of the Ni alloying element led to increased IMC layer thickness, the overall reaction layers were roughly 60 μm.

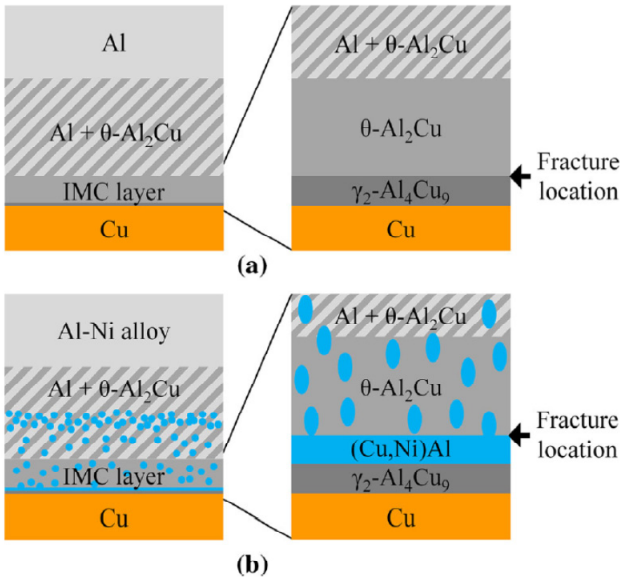

Figure 19. Schematic illustration of the Al/Cu dissimilar interface and fracture location of the joint produced (a) without alloying elements and (b) with the addition of Ni to Al. Reproduced from Ref. [55] with the permission.

Shi et al. [120] studied the effect of filler wires in the pulsed double electrode gas arc welding Al 1060–Cu, and concluded that the Si element can reduce the diffusion of Al and Cu atoms thus the formation of IMCs. Also, Weigl et al. [58] studied the effect of Si in filler wires of AlSi12 and CuSi3. The results indicate that the silicon element increases the fluidity of the molten metal and therefore produces a uniform intermixture of elements during the welding process. As a result, the local formation of intermetallic in the Cu side in the transition zone of the weld zone was specifically reduced. Using AlSi12 exhibits negligible micro-cracking and better bending deformation. Application of AlSi12 is recommended to reach enhanced mechanical properties especially tensile strength due to a higher level of Si than CuSi3 in laser welding of Al–Cu [58].

In the case of laser welding of Al and Cu plate using Sn foil (i.e., SnAgTi) [84] shows a uniform and ductile fracture. This can be attributed to the formation of a ductile ternary Al–Ag–Cu alloy and also less and uniform intermixture of Al in Cu and Cu on the Al side.

In the case of brazing of Al alloys with the application of AlCuSi filler metal, thermally sprayed AlCuSi layer, and AlCuSi(Mg) filler metal, important parameters to have a metallurgical bond are direct contact of joints partners, Mg content, and the brazing window (see Figures 20 and 21). After joining, no magnesium was detectable in the braze metal because the magnesium in the filler metal completely sublimes during the brazing cycle and acts as a getter for oxygen and water vapor and thus improving the brazing atmosphere and formation of a brazed joint. Some copper diffusion into the aluminum base metal is assumed, and, therefore, the liquidus temperature of the filler metal is enhanced [47].

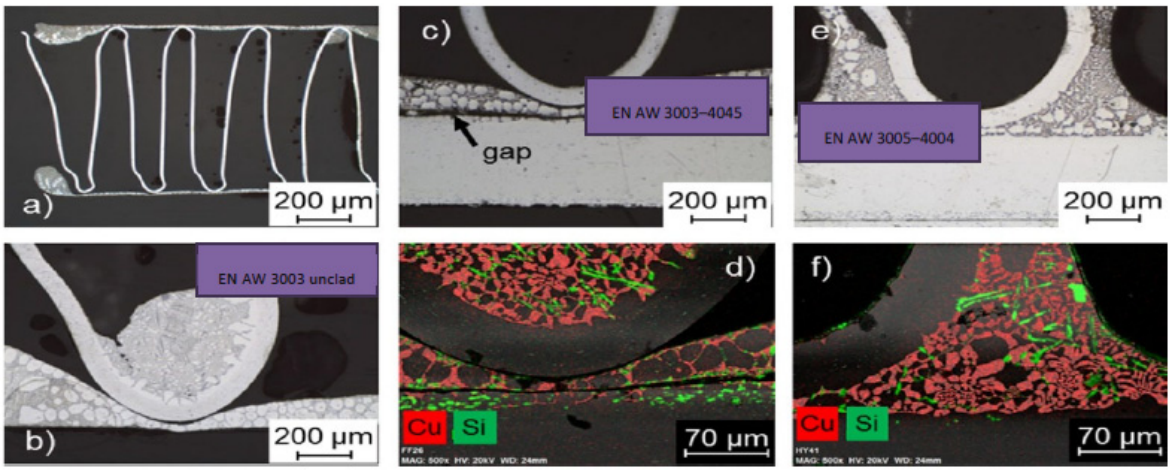

Figure 20. Sound brazing of Aluminum alloys with the application of AlCuSi filler metal. (a,b) EN AW-3003 unclad, (c,d) EN AW-3003/4045, and (e,f) EN AW-3005/4004. Reproduced from Ref. [47] with the permission.

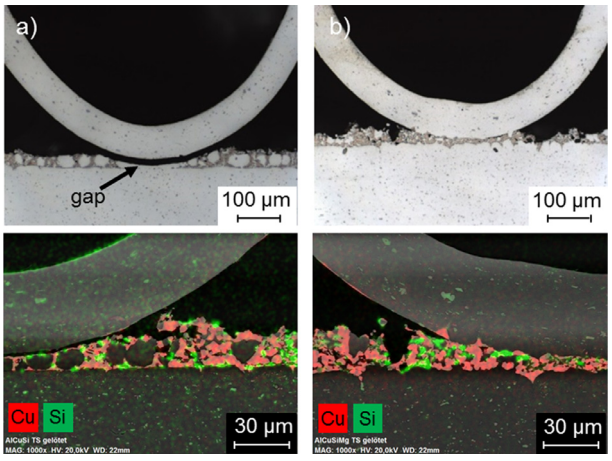

Figure 21. The figure shows the cross-sections of the brazed segments using the thermally sprayed AlCuSi (a) vs. AlCuSi (Mg) (b) filler metal. Image (b) shows sound brazing Al–Al joint with the application of AlCuSiMg filler metal. Reproduced from Ref. [47] with the permission.

9. Summary and conclusion

The laser welding of dissimilar materials aluminum sheet to the copper sheet in the busbar to battery tab joints is the main interest in this paper. The current review paper provides an adequate understating of the important factors influencing the Al–Cu busbar to battery tabs joint properties with laser welding and laser brazing of busbars to battery tabs, the formation, and growth of intermetallic compounds (IMCs) layer, mechanical properties of battery joints, electrical properties of the joint, long-term properties and finally how to enhance the joint properties.

1xxx series (e.g., 1050) and 3003 aluminum alloy and pure Copper plates with different purity grades such as 99.9% (electrolytic) and 99.995% (oxygen-free high-conductivity) or Ni-plated pure copper with thicknesses in the range of a few hundred micrometers up to a few millimeters are commonly used in the laser welding of busbar and battery tab. Laser welding and laser brazing of Al to Al and Al to Cu improved the joint properties, cost efficiency, and productivity in comparison to other common welding techniques.

In the case of welding dissimilar materials copper to aluminum, weak weld joint, porosity formation, HAZ degradation, hot cracking, cold cracks as well as the risk of IMC formation can cause difficulty. Additionally, different thermophysical properties of the joint metals such as melting temperature and thermal conductivity may restrict the weldability. A large part of the current review defines how the defects form such as IMCs and porosities during and after laser welding. The effect of materials properties in laser welding and laser brazing is discussed in detail. To avoid these defects and reach a sound laser welded joint of Al–Cu alloys, some measures such as laser welding speed, laser power, and power density, key-hole dynamic, shielding gas, should be taken.

Laser-materials interaction during the laser welding process has been observed to strongly affects the defect formation and therefore the joint properties. Laser-materials interaction can be influenced by process parameters adjustment (e.g., laser power and speed), laser operational mode, and choice of materials (e.g., base metals, alloying elements, filler metals, etc.). The currect combination of the above-mentioned items reduces the defects such as IMCs and hence enhances the joint properties in terms of mechanical and electrical properties.

By using optimal oscillation parameters such as wobbling pattern and amplitude, the metallurgical formation of these intermetallic phases in the weld can be specifically controlled and weld defects can be minimized. This enables to achieve higher values of mechanical properties with the required electrical and thermal conductivity. Application of laser beam oscillation can also reduce pores and process emissions such as spatter and melt ejections, and other defects such as weld cracking at low linear welding speeds. A proper process parameter window with altering the different pulse parameters (e.g., pulse shape and pulse time) may result in proper joint properties.

Different filler wires and alloying elements indicate that the brittle IMCs at the interface of two metals can be substituted with phases showing higher mechanical properties. For example, a ductile fracture of brazed of Al 1050 to Cu–OF using Cu–Ni–Sn–P brazing filler metal was reported. The formation of a ductile ternary alloy due to the application of a filler material that has a metallurgical affinity to aluminum and copper base metals such as nickel, silver, and tin may improve the joint properties. These alloys may enhance the mechanical properties of the joint. Also, some other investigations show that the addition of alloying elements to the Al/Cu joint can enhance the mechanical properties of the joint e.g., application of Al–Si and Al–Cu–Zn filler wires, as well as Ni and Sn foil (SnAgTi). As well using the AlSi12 exhibits a reduced local formation of intermetallic in

the Cu side in the transition zone of the weld zone and negligible micro-cracking and better bending deformation. Application of AlSi12 is recommended to reach enhanced mechanical properties especially tensile strength due to a higher level of Si. Also, the joint in long-term applications may result in a larger IMC layer due to electrical and thermal aging however in different growth behavior.

Acknowledgments

This paper was prepared under the EMPIRE project. We would like to acknowledge Vinnova and the strategic innovation programme for Metallic material for funding the EMPIRE project.

Conflict of interest

There is no conflict of interest between the authors.

References

1. Curry C, Bloomberg New Energy Finance, 2017. Lithium-ion battery costs and market.
2. Bloomberg New Energy Finance, 2020. Electric Vehicle Outlook. Available from: https://about.bnef.com/electric-vehicle-outlook/.
3. HS Markit, 2020. The battery electric vehicle: Why mass adoption is inevitable, yet elusive.
4. Samsung SDI. The Composition of EV Batteries: Cells? Modules? Packs? Let's Understand Properly! Available from: https://www.samsungsdi.com/column/all/detail/54344.html?listType=&pageIndex=1&searchCondition=&searchKeyword=&idx=54344.
5. Babbitt CW (2020) Sustainability perspectives on lithium-ion batteries. *Clean Technol Envir* 22: 1213–1214. https://doi.org/10.1007/s10098-020-01890-3
6. Richa K, Babbitt CW, Gaustad G (2017) Eco-efficiency analysis of a lithium-ion battery waste hierarchy inspired by circular economy. *J Ind Ecol* 21: 715–730. https://doi.org/10.1111/jiec.12607
7. Liu WW, Zhang H, Liu LH, et al. (2016) Remanufacturing cathode from end-of-life of lithium-ion secondary batteries by Nd:YAG laser radiation. *Clean Technol Envir* 18: 231–243. https://doi.org/10.1007/s10098-015-1010-1
8. Zwicker MFR, Moghadam M, Zhang W, et al. (2020) Automotive battery pack manufacturing-a review of battery to tab joining. *J Adv Joi Process* 1: 100017. https://doi.org/10.1016/j.jajp.2020.100017
9. Das A, Li D, Williams D, et al. (2018) Joining technologies for automotive battery systems manufacturing. *World Electr Veh J* 9: 22. https://doi.org/10.3390/wevj9020022
10. Shui L, Chen F, Garg A, et al. (2018) Design optimization of battery pack enclosure for electric vehicle. *Struct Multidisc Optim* 58: 331–347. https://doi.org/10.1007/s00158-018-1901-y
11. Lee JH, Lee HM, Ahn S (2003) Battery dimensional changes occurring during charge/discharge cycles-thin rectangular lithium ion and polymer cells. *J Power Sources* 119–121: 833–837. https://doi.org/10.1016/S0378-7753(03)00281-7
12. Zhao N, Zhao D, Xu L, et al. (2014) A multimode responsive aptasensor for adenosine detection. *J Nanomater* 2014: 1–7. https://doi.org/10.1155/2014/360347

13. Fleckenstein M, Bohlen O, Roscher MA, et al. (2011) Current density and state of charge inhomogeneities in Li-ion battery cells with $LiFePO_4$ as cathode material due to temperature gradients. *J Power Sources* 196: 4769–4778. https://doi.org/10.1016/j.jpowsour.2011.01.043
14. Yang N, Zhang X, Shang B, et al. (2016) Unbalanced discharging and aging due to temperature differences among the cells in a lithium-ion battery pack with parallel combination. *J Power Sources* 306: 733–741. https://doi.org/10.1016/j.jpowsour.2015.12.079
15. Wang Q, Ping P, Zhao X, et al. (2012) Thermal runaway caused fire and explosion of lithium ion battery. *J Power Sources* 208: 210–224. https://doi.org/10.1016/j.jpowsour.2012.02.038
16. Baumann M, Wildfeuer L, Rohr S, et al. (2018) Parameter variations within Li-ion battery packs-Theoretical investigations and experimental quantification. *J Energy Storage* 18: 295–307. https://doi.org/10.1016/j.est.2018.04.031
17. Baumhöfer T, Brühl M, Rothgang S, et al. (2014) Production caused variation in capacity aging trend and correlation to initial cell performance. *J Power Sources* 247: 332–338. https://doi.org/10.1016/j.jpowsour.2013.08.108
18. Brand MJ, Schmidt PA, Zaeh MF, et al. (2015) Welding techniques for battery cells and resulting electrical contact resistances. *J Energy Storage* 1: 7–14. https://doi.org/10.1016/j.est.2015.04.001
19. Hesse T, Zaske S (2018) A "World Champion" in Energy Efficiency: Environmental audit sees laser welding ahead of resistance spot welding. *Laser Tech J* 15: 56–58. https://doi.org/10.1002/latj.201800014
20. Kohn S, Berdichevsky G, Hewett BC (2011) Tunable frangible battery pack system. US Patent 7923144B2.
21. Shin HS, de Leon M (2017) Mechanical performance and electrical resistance of ultrasonic welded multiple Cu–Al layers. *J Mater Process Tech* 241: 141–153. https://doi.org/10.1016/j.jmatprotec.2016.11.004
22. Lee SS, Kim TH, Hu SJ, et al. (2010) Joining technologies for automotive lithium-ion battery manufacturing: A review. ASME 2010 International Manufacturing Science and Engineering Conference (MSEC 2010), Erie, Pennsylvania, USA, 1: 541–549. https://doi.org/10.1115/MSEC2010-34168
23. Wagner G, Balle F, Eifler D (2012) Ultrasonic welding of hybrid joints. *JOM* 64: 401–406. https://doi.org/10.1007/s11837-012-0269-5
24. Chamberlain A, Larsson H, Nilsson L, et al. (2019) Welding methods for electrical connections in battery systems. Uppsala University.
25. Das A, Ashwin TR, Barai A (2019) Modelling and characterisation of ultrasonic joints for Li-ion batteries to evaluate the impact on electrical resistance and temperature raise. *J Energy Storage* 22: 239–248. https://doi.org/10.1016/j.est.2019.02.017
26. McGovern ME, Rinker TJ, Sekol RC (2019) Assessment of ultrasonic welds using pulsed infrared thermography. *JNDE* 2: 011009. https://doi.org/10.1115/1.4042260
27. Mohan Raj N, Kumaraswamidhas LA, Nalajam PK, et al. (2018) Studies on electro mechanical aspects in ultrasonically welded Al/Cu joints. *Trans Indian Inst Met* 71: 107–116. https://doi.org/10.1007/s12666-017-1140-8
28. Choi S, Fuhlbrigge T, Nidamarthi S (2012) Vibration analysis in robotic ultrasonic welding for battery assembly. 2012 IEEE International Conference on Automation Science and Engineering (CASE), Seoul, Korea, 550–554. https://doi.org/10.1109/CoASE.2012.6386349

29. Kang B, Cai W, Tan CA (2014) Dynamic stress analysis of battery tabs under ultrasonic welding. *J Manuf Sci Eng* 136: 041011. https://doi.org/10.1115/1.4026990
30. Zhao J, Li H, Choi H, et al. (2013) Insertable thin film thermocouples for in situ transient temperature monitoring in ultrasonic metal welding of battery tabs. *J Manuf Process* 15: 136–140. https://doi.org/10.1016/j.jmapro.2012.10.002
31. Li H, Choi H, Ma C, et al. (2013) Transient temperature and heat flux measurement in ultrasonic joining of battery tabs using thin-film microsensors. *J Manuf Sci Eng* 135: 051015. https://doi.org/10.1115/1.4024816
32. Zhang H, Senkara J (2011) *Resistance Welding: Fundamentals and Applications*, 2 Eds., CRC Press. https://doi.org/10.1201/b11752
33. Saariluoma H, Piiroinen A, Unt A, et al. (2020) Overview of optical digital measuring challenges and technologies in laser welded components in EV battery module design and manufacturing. *Batteries* 6: 47. https://doi.org/10.3390/batteries6030047
34. Mehta KP, Badheka VJ (2016) A review on dissimilar friction stir welding of copper to aluminum: Process, properties, and variants. *Mater Manuf Process* 31: 233–254. https://doi.org/10.1080/10426914.2015.1025971
35. Mypati O, Mishra D, Sahu S, et al. (2020) A study on electrical and electrochemical characteristics of friction stir welded lithium-ion battery tabs for electric vehicles. *J Electron Mater* 49: 72–87. https://doi.org/10.1007/s11664-019-07711-8
36. Li W, Wen Q, Yang X, et al. (2017) Interface microstructure evolution and mechanical properties of Al/Cu bimetallic tubes fabricated by a novel friction-based welding technology. *Mater Design* 134: 383-393. https://doi.org/10.1016/j.matdes.2017.08.065
37. Brand MJ, Berg P, Kolp EI, et al. (2016) Detachable electrical connection of battery cells by press contacts. *J Energy Storage* 8: 69–77. https://doi.org/10.1016/j.est.2016.09.011
38. Bolsinger C, Zorn M, Birke KP (2017) Electrical contact resistance measurements of clamped battery cell connectors for cylindrical 18650 battery cells. *J Energy Storage* 12: 29–36. https://doi.org/10.1016/j.est.2017.04.001
39. Taheri P, Hsieh S, Bahrami M (2011) Investigating electrical contact resistance losses in lithium-ion battery assemblies for hybrid and electric vehicles. *J Power Sources* 196: 6525–6533. https://doi.org/10.1016/j.jpowsour.2011.03.056
40. Fu R, Choe SW, Jackson RL, et al. (2012) Modeling and analysis of vibration-induced changes in connector resistance of high power electrical connectors for hybrid vehicles. *Mech Based Des Struc* 40: 349–365. https://doi.org/10.1080/15397734.2012.670098
41. American Welding Society (1982) *Welding Handbook: Metals and Their Weldability*, 7 Eds. https://www.amazon.com/Welding-Handbook-Metals-Their-Weldability/dp/0871712180.
42. Davis JR, Ferutz K, Wheaton N (1980) *Asm Handbook: Welding, Brazing, and Soldering*, ASM International, 6.
43. American Welding Society (1991) *Brazing Handbook*, 4 Eds..
44. Hayashi J, Miyazawa Y (2014) Spot brazing of aluminum to copper with a cover plate. *IOP Conf Ser-Mater Sci Eng* 61: 012015. https://doi.org/10.1088/1757-899X/61/1/012015
45. Solchenbach T, Plapper P, Cai W (2014) Electrical performance of laser braze-welded aluminum-copper interconnects. *J Manuf Process* 16: 183–189. https://doi.org/10.1016/j.jmapro.2013.12.002

46. Brand MJ, Kolp EI, Berg P, et al. (2017) Electrical resistances of soldered battery cell connections. *J Energy Storage* 12: 45–54. https://doi.org/10.1016/j.est.2017.03.019
47. Sommer AK, Türpe M, Füssel U, et al. (2020) Considerations on a new brazing concept for vacuum brazing of aluminium and copper. *Weld World* 64: 1589–1596. https://doi.org/10.1007/s40194-020-00935-x
48. Krishnaja D, Cheepu M, Venkateswarlu D (2018) A review of research progress on dissimilar laser weld-brazing of automotive applications. *IOP Conf Ser-Mater Sci Eng* 330: 012073. https://doi.org/10.1088/1757-899X/330/1/012073
49. Markovits T, Jászberényi A (2018) Investigation of laser-material interaction in case of aluminium brazing process. *Period Polytech Transp Eng* 46: 59–62. https://doi.org/10.3311/PPtr.11528
50. Li Y, Chen C, Yi R, et al. (2020) Review: Special brazing and soldering. *J Manuf Process* 60: 608–635. https://doi.org/10.1016/j.jmapro.2020.10.049
51. Xiao R, Dong P (2011) Laser penetration brazing of dissimilar alloys. *International Congress on Applications of Lasers & Electro-Optics*, Orlando, Florida, USA, 2011: 308–314. https://doi.org/10.2351/1.5062251
52. Deyev G, Deyev D (2005) *Surface Phenomena in Fusion Welding Processes*, 1 Ed., CRC Press. https://doi.org/10.1201/9781420036299-1
53. Zhou L, Luo LY, Tan CW, et al. (2018) Effect of welding speed on microstructural evolution and mechanical properties of laser welded-brazed Al/brass dissimilar joints. *Opt Laser Technol* 98: 234–246. https://doi.org/10.1016/j.optlastec.2017.08.004
54. Xia C, Li Y, Puchkov UA, et al. (2008) Microstructure and phase constitution near the interface of Cu/Al vacuum brazing using Al–Si filler metal. *Vacuum* 82: 799–804. https://doi.org/10.1016/j.vacuum.2007.11.007
55. Furuya HS, Sato YS, Kokawa H, et al. (2018) Improvement of interfacial strength with the addition of Ni in Al/Cu dissimilar joints produced via laser brazing. *Metall Mater Trans A* 49: 6215–6223. https://doi.org/10.1007/s11661-018-4938-z
56. Sun Z, Ion JC (1995) Laser welding of dissimilar metal combinations. *J Mater Sci* 30: 4205–4214. https://doi.org/10.1007/BF00361499
57. Steen WM (1987) *Lasers in Manufacturing: Proceedings of the 4th International Conference, Birmingham*, UK, Kempston, Bedford: IFS Publications; Berlin, New York: Springer-Verlag, 12–14.
58. Weigl M, Albert F, Schmidt M (2011) Enhancing the ductility of laser-welded copper-aluminum connections by using adapted filler materials. *Physics Procedia* 12: 332–338. https://doi.org/10.1016/j.phpro.2011.03.141
59. Sun Z, Moisio T (1993) Laser beam welding of austenitic/ferritic dissimilar steel joints using nickel based filler wire. *Mater Sci Tech* 9: 603–608. https://doi.org/10.1179/mst.1993.9.7.603
60. 60. Kancharla V, Mendes M, Grupp M, et al. (2018) Recent advances in fiber laser welding. *Biul Inst Spawal Gliwicach* 62: 175–181. https://doi.org/10.17729/ebis.2018.5/20
61. 61. Blecher JJ, Galbraith CM, Van Vlack C, et al. (2014) Real time monitoring of laser beam welding keyhole depth by laser interferometry. *Sci Technol Weld Joi* 19: 560–564. https://doi.org/10.1179/1362171814Y.0000000225
62. Vasudevan AK, Doherty RD (1989) *Aluminum Alloys-Contemporary Research and Applications*, Boston: Academic Press.

63. Katgerman L, Soetens F (2010) New frontiers in light metals. *Proceedings of the 11th International Aluminium Conference INALCO 2010*, the Netherlands, 23–25.
64. Kah P, Rajan R, Martikainen J, et al. (2015) Investigation of weld defects in friction-stir welding and fusion welding of aluminium alloys. *Int J Mech Mater Eng* 10: 26. https://doi.org/10.1186/s40712-015-0053-8
65. Sun T, Franciosa P, Ceglarek D (2021) Effect of focal position offset on joint integrity of AA1050 battery busbar assembly during remote laser welding. *J Mater Res Technol* 14: 2715–2726. https://doi.org/10.1016/j.jmrt.2021.08.002
66. Kirchhoff M (2021) Welding: E-mobility, Trumpf Laser- und Systentechnik GmbH.
67. Laserline GmbH, 2021. Laserline LDblue welding of electrical copper connectors.
68. Kraetzsch M, Standfuss J, Klotzbach A, et al. (2011) Laser beam welding with high-frequency beam oscillation: Welding of dissimilar materials with brilliant fiber lasers. *Physics Procedia* 12: 142–149. https://doi.org/10.1016/j.phpro.2011.03.018
69. Dimatteo V, Ascari A, Fortunato A (2019) Continuous laser welding with spatial beam oscillation of dissimilar thin sheet materials (Al–Cu and Cu–Al): Process optimization and characterization. *J Manuf Process* 44: 158–165. https://doi.org/10.1016/j.jmapro.2019.06.002
70. Lerra F, Ascari A, Fortunato A (2019) The influence of laser pulse shape and separation distance on dissimilar welding of Al and Cu films. *J Manuf Process* 45: 331–339. https://doi.org/10.1016/j.jmapro.2019.07.015
71. Olowinsky A (2021) How Lasers improve battery production. Available from: https://www.ilt.fraunhofer.de/de/mediathek/vortraege.html.
72. Huang W, Wang H, Rinker T, et al. (2020) Investigation of metal mixing in laser keyhole welding of dissimilar metals. *Mater Design* 195: 109056. https://doi.org/10.1016/j.matdes.2020.109056
73. Schmalen P, Plapper P, Cai W (2016) Process robustness of laser braze-welded Al/Cu connectors. *SAE Int J Alt Power* 5: 195–204. https://doi.org/10.4271/2016-01-1198
74. Schmalen P, Plapper P (2016) Evaluation of laser braze-welded dissimilar Al–Cu joints. *Physics Procedia* 83: 506–514. https://doi.org/10.1016/j.phpro.2016.08.052
75. Reisgen U, Olschok S, Jakobs S, et al. (2018) Influence of the degree of dilution with laser beam vacuum-welded Cu–Al mixed joints on the electrical properties. *Procedia CIRP* 74: 23–26. https://doi.org/10.1016/j.procir.2018.08.022
76. Solchenbach T, Plapper P (2013) Mechanical characteristics of laser braze-welded aluminium-copper connections. *Optics Laser Technol* 54: 249–256. https://doi.org/10.1016/j.optlastec.2013.06.003
77. Britten SW, Schmid L, Molitor T, et al. (2020) Blue high-power laser sources for processing solutions in e-mobility and beyond. *Procedia CIRP* 94: 592–595. https://doi.org/10.1016/j.procir.2020.09.082
78. Zediker MS, Fritz RD, Finuf MJ, et al. (2020) Laser welding components for electric vehicles with a high-power blue laser system. *J Laser Appl* 32: 022038. https://doi.org/10.2351/7.0000054
79. Mathivanan K, Plapper P (2019) Laser welding of dissimilar copper and aluminum sheets by shaping the laser pulses. *Procedia Manuf* 36: 154–162. https://doi.org/10.1016/j.promfg.2019.08.021

80. Schmalen P, Plapper P (2017) Resistance measurement of laser welded dissimilar Al/Cu joints. *J Laser Micro Nanoen* 12: 189–194. https://doi.org/10.2961/jlmn.2017.03.0003
81. Schmalen P, Plapper P, Peral I, et al. (2018) Composition and phases in laser welded Al–Cu joints by synchrotron X-ray microdiffraction. *Procedia CIRP* 74: 27–32. https://doi.org/10.1016/j.procir.2018.08.006
82. Solchenbach T, Plapper P, Greger M, et al. (2014) Thermal and electrical aging of laser braze-welded aluminum-copper interconnects. *Transl Mater Res* 1: 015001. https://doi.org/10.1088/2053-1613/1/1/015001
83. Mathivanan K, Plapper PW (2019) Laser overlap joining from copper to aluminum and analysis of failure zone. *Lasers in Manufacturing Conference 2019*, Munich, Germany.
84. Hailat MM, Mian A, Chaudhury ZA, et al. (2012) Laser micro-welding of aluminum and copper with and without tin foil alloy. *Microsyst Technol* 18: 103–112. https://doi.org/10.1007/s00542-011-1378-8
85. Helm J, Dietz von Bayer I, Olowinsky A, et al. (2019) Influence of the surface properties of the connector material on the reliable and reproducible contacting of battery cells with a laser beam welding process. *Weld World* 63: 1221–1228. https://doi.org/10.1007/s40194-019-00727-y
86. Lee SJ, Nakamura H, Kawahito Y, et al. (2014) Effect of welding speed on microstructural and mechanical properties of laser lap weld joints in dissimilar Al and Cu sheets. *Sci Technol Weld Joi* 19: 111–118. https://doi.org/10.1179/1362171813Y.0000000168
87. Risdiyanto A, Arifin M, Khayam U (2013) Study on temperature distribution at busbar connection based on contact resistance of different plating contact surface. *2013 Joint International Conference on Rural Information & Communication Technology and Electric-Vehicle Technology (rICT & ICeV-T)*, Bandung, Indonesia. https://doi.org/10.1109/rICT-ICeVT.2013.6741537
88. Farahat MA, Gockenbach E, El-Alaily AA, et al. (1996) Effect of coating materials on the electrical performance of copper joints. *Proceedings of the Forty-Second IEEE Holm Conference on Electrical Contacts*, 472–478. https://doi.org/10.1109/HOLM.1996.557229
89. Wong TT, Liang GY, An G, et al. (2005) The electrical conductivity of laser-remelted and plasma-sprayed Ni and Cr coatings. *J Mater Process Tech* 159: 265–271. https://doi.org/10.1016/j.jmatprotec.2004.05.012
90. Swedish Institute of Standards (2016) Aluminum and aluminum alloy-Sheet metal and strip-Part 2: Mechanical properties. SS-EN 485-2.
91. ASM Handbook Committee (1990) Properties and selection: Nonferrous alloys and special-purpose materials, *ASM Handbook*, ASM International, 2.
92. Swedish Institute of Standards (2019) Aluminium and aluminium alloys—Chemical composition and form of wrought products-Part 3: Chemical composition and form of products. SS-EN 573-3.
93. Solchenbach T, Plapper P (2013) Combined laser beam braze-welding process for fluxless Al–Cu connections. *International Conference on competitive Manufacturing (COMA)*, 13: 131–136.
94. Kah P, Vimalraj C, Martikainen J, et al. (2015) Factors influencing Al–Cu weld properties by intermetallic compound formation. *Int J Mech Mater Eng* 10: 10. https://doi.org/10.1186/s40712-015-0037-8

95. Lee YG, Duh JG (1998) Characterizing the formation and growth of intermetallic compound in the solder joint. *J Mater Sci* 33: 5569–5572. https://doi.org/10.1023/A:1004499728840
96. Mys I, Schmidt M (2006) Laser micro welding of copper and aluminum. *Lasers and Applications in Science and Engineering*, San Jose, California, United States, 610703. https://doi.org/10.1117/12.648376
97. Watanabe W, Onda S, Tamaki T, et al. (2006) Space-selective laser joining of dissimilar transparent materials using femtosecond laser pulses. *Appl Phys Lett* 89: 021106. https://doi.org/10.1063/1.2221393
98. Braunovic M (2007) Reliability of power connections. *J Zhejiang Univ-Sc A* 8: 343–356. https://doi.org/10.1631/jzus.2007.A0343
99. Kaplan AFH (2005) Model of the absorption variation during pulsed laser heating applied to welding of electronic Au/Ni-coated Cu-leadframes. *Appl Surf Sci* 241: 362–370. https://doi.org/10.1016/j.apsusc.2004.07.035
100. Huntington CA, Eagar TW (1983) Laser welding of aluminum and aluminum alloys. *Weld Res Suppl* 62: 105–107.
101. Kannatey-Asibu Jr E (2009) *Principles of Laser Materials Processing*, John Wiley & Sons. https://doi.org/10.1002/9780470459300
102. Delgado-Pinar M, Zalvidea D, Diez A, et al. (2006) Q-switching of an all-fiber laser by acousto-optic modulation of a fiber Bragg grating. *Opt Express* 14: 1106. https://doi.org/10.1364/OE.14.001106
103. Heider A, Weber R, Herrmann D, et al. (2015) Power modulation to stabilize laser welding of copper. *J Laser Appl* 27: 022003. https://doi.org/10.2351/1.4906127
104. Minasian RA (2005) MODULATORS|modulation and demodulation of optical signals, In: Guenther CD, *Encyclopedia of Modern Optics*, Elsevier, 129–138. https://doi.org/10.1016/B0-12-369395-0/00667-9
105. Purdue University, Modulation of light. Available from: https://www.physics.purdue.edu/webapps/index.php/course_document/index/phys570P/1684/25/14317
106. Markettech, 2008. Overview of modulated and pulsed diode laser systems. Available from: https://www.markettechinc.net/wp-content/uploads/2018/05/Modulated-and-Pulsed-Diode-Lasers.pdf.
107. Schiry M, Plapper P (2019) Novel opportunities by laser welding of dissimilar materials. *Proceedings of International Conference on Competitive Manufacturing COMA'19*, South Africa, 293–300.
108. Müller A, Goecke SF, Rethmeier M (2018) Laser beam oscillation welding for automotive applications. *Weld World* 62: 1039–1047. https://doi.org/10.1007/s40194-018-0625-3
109. Xue Z, Hu S, Zuo D, et al. (2013) Molten pool characterization of laser lap welded copper and aluminum. *J Phys D Appl Phys* 46: 495501. https://doi.org/10.1088/0022-3727/46/49/495501
110. Deyneka-Dupriez N, Denkel A (2020) For a better world: OCT unlocks real-time quality control during oscillation welding. Lessmüller Lasertechnik. Available from: https://www.lasersystemseurope.com/analysis-opinion/better-world-oct-unlocks-real-time-quality-control-during-oscillation-welding.
111. Müller A, Goecke SF, Sievi P, et al. (2014) Laser beam oscillation strategies for fillet welds in lap joints. *Physics Procedia* 56: 458–466. https://doi.org/10.1016/j.phpro.2014.08.149

112. Dimatteo V, Ascari A, Fortunato A (2021) Dissimilar laser welding of copper and aluminum alloys in multilayer configuration for battery applications. *J Laser Appl* 33: 042028. https://doi.org/10.2351/7.0000476
113. Wahba M, Kawahito Y, Katayama S (2011) Laser direct joining of AZ91D thixomolded Mg alloy and amorphous polyethylene terephthalate. *J Mater Process Tech* 211: 1166–1174. https://doi.org/10.1016/j.jmatprotec.2011.01.021
114. Schmidt PA, Pauleser T, Zaeh MF (2014) Optimisation of weld seam configurations using a genetic algorithm. *Procedia CIRP* 25: 393–399. https://doi.org/10.1016/j.procir.2014.10.054
115. Mai TA, Spowage AC (2004) Characterisation of dissimilar joints in laser welding of steel-kovar, copper-steel and copper-aluminium. *Mater Sci Eng-A Struct* 374: 224–233. https://doi.org/10.1016/j.msea.2004.02.025
116. Cai ZP, Ai BQ, Cao R, et al. (2016) Microstructure and properties of aluminum AA6061-T6 to copper (Cu)-T2 joints by cold metal transfer joining technology. *J Mater Res* 31: 2876–2887. https://doi.org/10.1557/jmr.2016.295
117. Mehta KP, Badheka VJ (2017) Hybrid approaches of assisted heating and cooling for friction stir welding of copper to aluminum joints. *J Mater Process Tech* 239: 336–345. https://doi.org/10.1016/j.jmatprotec.2016.08.037
118. Esser G, Mys I, Schmidt MH (2004) Laser micro welding of copper and aluminium using filler materials. *Fifth International Symposium on Laser Precision Microfabrication* 5662: 337–342. https://doi.org/10.1117/12.596330
119. Tavassoli S, Abbasi M, Tahavvori R (2016) Controlling of IMCs layers formation sequence, bond strength and electrical resistance in Al–Cu bimetal compound casting process. *Mater Design* 108: 343–353. https://doi.org/10.1016/j.matdes.2016.06.076
120. Shi Y, Zhou XL, Zhu M, et al. (2017) Effect of filler wires on brazing interface microstructure and mechanical properties of Al/Cu dissimilar metals welding-brazing joint. *Mater Rep* 31: 61–64 (in Chinese).

AIMS Press